GRANT/ AMES 60 pages

C.R

IN-
26387

SEMI-ANNUAL TECHNICAL REPORT

for

NASA Grant No. NAG2-315

Entitled: "A SIRTF INTERDISCIPLINARY SCIENTIST PROPOSAL"

Submitted by

THE REGENTS OF THE UNIVERSITY OF CALIFORNIA
UNIVERSITY OF CALIFORNIA, LOS ANGELES
DEPARTMENT OF ASTRONOMY
405 HILGARD AVENUE
LOS ANGELES, CALIFORNIA 90024

Period Covered by Report: April 1, 1986 - September 12, 1986

PRINCIPAL INVESTIGATOR:

Professor Edward L. Wright
Department of Astronomy
Telephone No. (213) 825-5755

(NASA-CR-176862) A SIRTF INTERDICIPLINARY SCIENTIST PROPOSAL Semiannual Technical Report, 1 Apr. - 12 Sep. 1986 (California Univ.) 60 p CSCL 03B

N86-32382

Unclas
G3/90 43543

SEMI-ANNUAL REPORT FOR SIRTF 9/12/86

From: Edward L. Wright, UCLA Dept. of Astronomy

The paper "Effect of Intervening Galaxies on Quasar Counts and Colors", by Edward L. Wright, has been accepted by the **Astrophysical Journal.** Another paper on quasars counts, "Source Counts in the Chronometric Cosmology", by Edward L. Wright, has been submitted to and accepted by the **Astrophysical Journal.** A copy of this manuscript is enclosed. The paper "The R/IR Evolution in Galaxies - Effect of the Stars on the AGB", by Arati Choksi and Edward L. Wright, has been submitted to the **Astrophysical Journal.** A copy of this manuscript is enclosed. In addition, I presented a poster paper at the IRAS meeting in Pasadena, "Using SIRTF to Study Extragalactic Star Formation", by Edward L. Wright.

I have also attended one Science Working Group meetings, and organized one meeting of the Ned Wright Committee. A large amount of Ned Wright Committee work has taken place by TELEMAIL.

SOURCE COUNTS IN THE CHRONOMETRIC COSMOLOGY

by

Edward L. Wright

UCLA Department of Astronomy

Los Angeles, CA 90024

RECEIVED: 1986 April 28;

ABSTRACT

The chronometric cosmology (a static, homogeneous and hence non-evolving model proposed by Segal) is unable to explain the steep number *vs*. flux law N(S) for quasars or extragalactic radio sources. The explanation given by Segal (1976) to explain the steep N(S) laws gives at best a small increase over a Euclidean $N(S) \propto S^{-1.5}$, and requires that the source spectral index α be close to but greater than zero to create the effect (where $F_\nu \propto \nu^{-\alpha}$). For typical radio spectral indices $\alpha \simeq 0.75$, the chronometric model cannot give a quantitative fit to the excess number of 1-3 Jy sources that the standard cosmology attributes to evolution. Thus the chronometric model can explain a steep N(S) law only for flat spectrum sources, while the observations show the steepest N(S) law for steep spectrum sources. Furthermore, the observed N(S) law for ultraviolet excess quasars is steeper than the steepest possible chronometric prediction. The agreement between the chronometric theory and the quasar counts claimed by Segal, Loncaric and Segal (1980) and Segal and Nicoll (1986) is a side effect of the restricted redshift range used by these authors, rather than a correct prediction by the

chronometric theory.

Subject Headings: cosmology - quasars - radio Sources: general - radio sources: spectra

INTRODUCTION

Source counts provide one of the strongest indications that the Universe has evolved from a more active state in the past to a quieter present. They have been used as evidence against cosmological models that propose an unchanging Universe, for example the Steady State. Such models predict a number vs. flux law that is less steep than the Euclidean $S^{-1.5}$ relation, while the observed radio counts follow a steeper $S^{-1.8}$ law for bright sources. The standard Friedmann models without evolution have the same deficiency, but in an evolving Universe an evolving source density is logically consistent. The chronometric model proposed by Segal (1976) is a static, homogeneous, nonevolving cosmology, so one would expect the same difficulties with $N(S)$ would arise; but Segal gives a qualitative argument that suggests that the radio source counts could be reproduced for sources with spectral index $\alpha < 1$. This paper makes a quantitative calculation to find out how much less than one the spectral index must be for the chronometric prediction to match the 408 MHz source counts in Wall, Pearson and Longair (1980). The same method is then used to compare counts of optically selected quasistellar objects with the chronometric prediction. I find that the good fit of the quasar counts by the chronometric theory claimed by Segal, Loncaric and Segal (1980, hereafter SLS) and Segal and Nicoll (1986) is due to their redshift cutoff and not to the chronometric theory.

CALCULATION

Segal's (1976) chronometric cosmology is based on a static Universe with a spherical geometry for space. The distance is given by

$$d = \theta R \tag{1}$$

where R is the radius of the Universe. The redshift in this model is due to differences between the two generators of time-like translations in the conformal group O(4,2): it is not caused by expansion. The most remarkable prediction of the chronometric cosmology is that the redshift follows the square of the distance for small distances:

$$z = \tan^2(\theta/2) \tag{2}$$

The chronometric cosmology predicts the following redshift-flux law for power law sources:

$$F_\nu = (L_\nu/16\pi R^2)(1+z)^{2-\alpha}/z \tag{3}$$

The volume-redshift law is given by:

$$dV/dz = 16\pi R^3 z^{0.5}/(1+z)^3. \tag{4}$$

The qualitative explanation for the excess of medium flux sources involves the redshift-flux law, which for $\alpha < 1$ reaches a minimum flux F_{min} at a redshift z_{min}, then rises for larger redshifts. Thus a source can appear bright either by being close to the observer or close to the antipode where $\theta = \pi$ and $z = \infty$. This produces a large number of sources with fluxes near F_{min}, which can explain the excess of medium flux sources over the Euclidean expectation. The magnitude of this effect depends on α, however, and it is never very large. Figure 1 shows a plot of $S^{3/2}N(>S)$ vs. S for $\alpha = -0.25$, 0, 0.25, 0.5, 0.75 and 1.00. As α approaches 0^+ the rise above Euclidean increases until it abruptly falls when $\alpha \leq 0$.

The rise above the Euclidean law does not continue to increase with decreasing α after $\alpha = 0$ because for $\alpha < 0$ the high redshift region giving an apparently bright source becomes larger than the low redshift region giving an equally bright source. The volume-redshift law has the property that the volume with redshift < z is the same as the volume with redshift > 1/z. When α is negative, z_{min} is less than 1, and the region with $z > z_{min}$ has a larger volume than the region with $z < z_{min}$. Since the flux for $z >> z_{min}$ follows

$$F \propto z^{1-\alpha} \tag{5}$$

the volume with $z >> z_{min}$ that gives a flux > S goes like

$$V \propto z^{-1.5} \propto S^{-1.5/(1-\alpha)} \tag{6}$$

for $\alpha < 1$. Thus the high redshift region contributes an N(S) law that follows

$$N(S) \propto S^{-1.5/(1-\alpha)} \tag{7}$$

at high fluxes, which for $0 < \alpha < 1$ is steeper than Euclidean, as is required. But for $\alpha < 0$ this becomes less steep than Euclidean, as can be seen in the curve for $\alpha = -0.25$ in Figure 1. Models with $\alpha \leq 0$ in the chronometric cosmology are very improbable, since the brightest sources in these models are dominated by objects with

$z >> 1$, unlike any known sample.

This mechanism for explaining the steep N(S) law for radio sources has a definite limitation: the rise above a Euclidean law is always less than a small factor. To quantify the rise above Euclidean given by the chronometric model I will define a Euclidean excess ratio for the flux range $S_1 < S_2$ in a number vs. flux law N(S) as

$$E(S_1,S_2) = (S_1/S_2)^{1.5}\ N(S_1)/N(S_2) \tag{8}$$

This ratio can be calculated both for theoretical models and for observed counts. Theoretically E depends on the density of sources with spectral index α and luminosity L: $\rho(\alpha,L)$. But if ρ can be written as the sum of two non-negative functions $f(\alpha,L)$ and $g(\alpha,L)$,

$$\rho(\alpha,L) = f(\alpha,L) + g(\alpha,L) \tag{9}$$

with corresponding Euclidean excesses E_f and E_g such that

$$E_f \leq E_g, \tag{10}$$

then the Euclidean excess for ρ, E_ρ, satisfies

$$E_f \leq E_\rho \leq E_g. \tag{11}$$

This implies that the extreme values of E will always be attained by models with a single type of source, having

$$\rho(\alpha,L) = \delta(\alpha-\alpha_o)\ \delta(L-L_o). \tag{12}$$

For the chronometric cosmology the largest value of E for any α, S_1 and S_2 is $E_{max} = 3\pi/2$ in the limit $\alpha \to 0^+$, $S_1 = F_{min}$, and $S_2 \to \infty$.

Observationally E_{obs} is 17.21 for quasars in the flux range from 19.8th magnitude (35 quasars in 1.72 deg^2, Marshall _et al._, 1984) to 15.4th magnitude (29 quasars in 10,700 deg^2, Schmidt and Green, 1983), which is much greater than $3\pi/2$. The maximum E predicted by the chronometric model is less than $3\pi/2$ for a finite flux range, such as $S_2/S_1 = 58$ corresponding to the 4.4 mag range for E_{obs}. Figure 2 shows E_{max} _vs._ S_2/S_1, and the chronometric model predicts $E \leq 3.3$ for this flux range.

Other non-evolving cosmologies, such as a non-evolving Friedmann model, the Steady State model, or the tired light model, do not produce any rise above Euclidean at all. This requires that $E_{max} = 1$ for these models. By contrast, an evolving cosmology has a source density that can depend on the redshift z as well, and E_{max} is infinity for a single type of source at a single redshift. Thus the chronometric cosmology can give a steeper N(S) law than other non-evolving models, but the observed quasar counts seem to rule out all the non-evolving cosmologies.

RADIO SOURCE COUNTS

A quantitative comparison of the chronometric model with the observed radio source counts depends on the luminosity function. Wall et al. use identifications of bright sources to construct a luminosity function, but this method depends on the cosmological model. I have used a more general approach in my calculations, by asking whether any positive luminosity function can fit the data. Thus I have performed a linear least-squares fit to the 408 MHz source counts using the values of the luminosity function in bins of width 0.1 in $\log_{10}L$ as parameters. The density of sources in each bin is constrained to be positive, so the problem can be solved by quadratic programming. To be specific, let the observations give N_i sources in solid angle Ω_i in the i^{th} flux bin, and let the model specify the density ρ_j of sources with luminosity L_j. Define V_{ij} as the volume/steradian in which a source with luminosity L_j would give a flux in the i^{th} flux bin. Then

$$\chi^2 = \sum_i \left(N_i - \Omega_i \sum_j V_{ij}\rho_j\right)^2 / N_i \tag{13}$$

and the calculation consists of minimizing χ^2 by varying the ρ_j subject to the constraint that $\rho_j \geq 0$. I have done this calculation many times with different values of the spectral index α.

Figure 3 shows the result of this calculation. The effect postulated by Segal can be seen as the χ^2 improves toward smaller α. The best value of χ^2 is 30, obtained when $\alpha = 0.19$. Since there are 24 flux bins in the Wall et al. data, this fit is acceptable, if one ignores the number of parameters fitted to the data. The actual calculations had 40 free parameters, defining the luminosity function over a $10^4:1$ range in luminosity; but the densities of only 12 bins were non-zero and truly free. Figure 4 shows the counts from Wall et al. compared with fits for three different values of α. The jagged structure in the model curves at low fluxes is real. It is caused by the sharp peaks in N(S) at $S = F_{min}$ for fixed luminosity, and the small bin width in my model luminosity functions. As a result the quadratic programming algorithm can give an exact fit to the low flux counts wherever N(S) is less steep than Euclidean. Thus the fairly good value of $\chi^2 = 30$ is obtained by a model which gives a mediocre fit to the steep N(S) at high fluxes. However, even if I assume every non-zero value of the luminosity function is a free parameter, $\chi^2 = 30$ with 12 degrees of freedom occurs 0.3% of the time from statistical fluctuations alone, which is similar to a 3 sigma fluctuation.

My interpretation of these results is that the fit to the source counts is marginally acceptable for $0.1 < \alpha < 0.4$. Wall et al., using a five parameter evolving luminosity function in the standard Big Bang cosmology, obtained $\chi^2 = 23.8$, which is somewhat better than the best chronometric model, and do not require unrealistic spectral indices. In an evolving model the "K corrections" to fluxes implied by different values of the spectral index can be absorbed into the luminosity evolution, so the χ^2 of the fit is independent of the assumed spectral index. Wall et al. actually used $\alpha = 0.75$. The observed spectral index distribution of sources selected at 408 Mhz has been measured by Katgert (1976), who gives $\langle\alpha\rangle = 0.79 \pm 0.024$ (sd of mean) for sources brighter than 5.5 Jy at 408 Mhz, and

$\langle\alpha\rangle = 0.87 \pm 0.028$ for a sample of 61 sources brighter than 0.06 Jy. For these measured values of α the best fitting chronometric model gives $\chi^2 > 140$ which is totally unacceptable.

Considering radio samples with known spectral indices makes the deficiency of the chronometric model most evident. Machalski (1978) gives counts from the the GB2 survey of sources with 408–1400 MHz spectral indices $\alpha > 1$. This steep spectrum sample shows an N(S) following

$$N = N_o S^{-\beta} \tag{14}$$

with $\beta = 1.90 \pm 0.11$. Figure 1 shows that the chronometric model will have $\beta < 1.5$ for $\alpha > 1$, so the chronometric model fails by 3.6 σ. For flat spectrum sources with $\alpha < 0.5$, which could have $\beta > 1.5$ in the chronometric model, Machalski finds that $\beta = 1.36 \pm 0.09$. Thus the chronometric cosmology can not explain the observed steepness of the steep spectrum source counts. It could explain a steep N(S) law for flat spectrum sources but this is not observed.

OPTICAL QSO COUNTS

Since the N(S) curve for optical quasars is much steeper than Euclidean, and is in fact steeper than the radio source counts, the limited ability of the chronometric cosmology to give steep source counts is quite inadequate to explain quasar counts. Figure 5 shows the quasar counts of Koo and Kron (1982), normalized to a Euclidean law with 2 quasars per square degree brighter than 18^{th} magnitude. The counts for bright quasars were read from Figure 7 in Koo and Kron, as was the luminosity evolution model of Braccesi *et al.* (1980). However, the points for $B < 16$ are from Schmidt and Green (1983), and the Green & Schmidt 1978 point has been replaced by two bins taken from Table 2 of Schmidt and Green (1983), using the counts for *all* objects, not the sample restricted to $M_B < -23$. By analyzing just the N(S) curve for quasars without using their redshifts, the radio source count calculation can be used without modification. But now the best fit, which is obtained with $\alpha = 0.15$, gives $\chi^2 = 69$ for 15 degrees of freedom, which is quite unacceptable. This best fitting chronometric model is plotted in Figure 5, and it is unable to match the observed N(S).

DISCUSSION

My conclusions about quasar counts in the chronometric cosmology are completely different from those reached by SLS and Segal and Nicoll (1986), and it is important to examine the causes of this disagreement. SLS present the theory of number counts in the chronometric cosmology in their section II, and explain the steepening of the number counts near F_{min}, in a manner that is completely consistent with this paper. However, in section III, "EMPIRICAL COMPARISON", SLS introduce a lower limit to redshifts, $z > z_1 = 0.1$, which is the actual reason their calculated N(S) is steep at high fluxes. In fact, the most luminous quasar in the SLS luminosity function would have $m = 15.5$ at $z = 0.1$, so SLS could predict an infinitely steep N(S) with no bright quasars at all. Thus when SLS conclude that the chronometric theory fits the quasar counts, this conclusion is not a consequence of their theoretical discussion, but rather a side effect of the apparently innocuous parameter z_1. Introducing a lower limit to redshifts will produce a steep N(S) law in any theory where flux is anti-correlated with redshift: for example, the N(S) law for galaxies with $z > 0.1$ is very steep near $B = 16$, but this is not a result of evolution.

The use of a restricted redshift range by SLS is a very strong assumption in the chronometric cosmology. For a fixed absolute magnitude, the total range of apparent magnitudes in the redshift range $0.1 < z < 4$ considered by Segal and Nicoll (1986) is only 1.62 mag for $\alpha = 0.5$, and only 1.31 mag for $\alpha = 0.15$. Contrast this with an $\Omega = 1$ Friedmann model which gives a range of 8.66 mag. Thus by limiting the redshift range Segal and Nicoll destroy the power of the

N(S) test, because apparently faint quasars must be intrinsically faint, while apparently bright quasars must be intrinsically luminous, and an arbitrary N(S) can be fit by adjusting the luminosity function. But the calculations in this paper show that a large number of bright quasars with $z < 0.1$ are predicted by any chronometric model that matches the quasar counts at 18-19th magnitude. Figure 6 shows a comparison of the Segal and Nicoll model (the extended RLF from their Table 7) with the quasar count data. To make this plot I have used $\alpha = 0.5$, and adjusted the count and flux normalization to best fit the peak and the sharp drop. By requiring $z > 0.1$ Segal and Nicoll get a fair fit over the range from 15.5 to 19th mag, and could fit all the data with a more extended luminosity function. But the predicted counts from the same model without the redshift restriction are ten times higher than the observed counts at the bright end.

Certainly some correction for the resolution of low redshift quasars into N galaxies and/or Seyferts must be made, but the redshift cutoff used by SLS does not match the de facto definition based on a stellar appearance on the POSS. Half of the quasars with $B < 15.4$ in the Schmidt and Green (1983) sample have $z < 0.1$. On the other hand, there is no difficulty in distinguishing galaxies from stellar objects down to 18^{th} magnitude on the POSS. Thus the abrupt redshift cutoff used by SLS rejects some true quasars and passes some true galaxies. The proper selection model would require a minimum difference between the magnitude of the nucleus and the magnitude of the underlying galaxy before accepting the nucleus as a quasar; and if this difference were independent of the magnitude of the galaxy then no redshift or magnitude dependent correction to the counts would be needed. The analysis by Yee (1983) of the ratio of the nuclear luminosity L_N to the galaxy luminosity L_G in Markarian galaxies shows that $L_N/L_G \leq 1$; while the study by Gehren, Fried, Wehinger and Wyckoff (1984) of fuzz around low redshift quasars shows that $L_N/L_G > 1$ for most quasars, and finds no trend of L_N/L_G with redshift. Thus it appears that a stellar appearance on the POSS requires $L_N/L_G > 1$ independent of redshift, so the resolution correction to quasar counts is negligible, and the results presented above eliminate the chronometric theory as a possible model of the Universe.

Schmidt and Green used a model dependent luminosity cutoff, $M_B < -23$, to define quasars, but I have analyzed their total sample without this cutoff. Some of these objects show associated nebulosity on the POSS: 50% of the objects with B < 15, and 14% of those with 15.4 < B < 15. Eliminating these slightly nebulous sources would make the quasar counts even steeper, and the fit to the chronometric model even worse.

CONCLUSIONS

Segal's chronometric cosmology provides an adequate fit to the radio source counts only for an unrealistic choice of spectral index. Since the typical observed spectral index of 0.75 gives a completely unacceptable $\chi^2 = 136$ with 24 (or fewer) degrees of freedom, I conclude that the actual Universe does not fit the chronometric model. Counts of ultraviolet excess quasistellar objects also show a steep N(S) curve that the chronometric cosmology cannot explain. Claims to the contrary by Segal, Loncaric, and Segal (1980) and Segal and Nicoll (1986) depend on a seemingly innocuous assumption that in fact destroys the power of the N(S) test. Even though the chronometric model gives a better fit than other non-evolving models (such as the Steady State, the tired light model of LaViolette (1986) or a non-evolving Friedmann model) it must be ruled out along with all non-evolving cosmologies.

This work was supported in part by grant number NAG2-315 from the NASA Ames Research Center.

REFERENCES

Braccesi, A., Zitelli, V., Bonoli, F., and Formiggini, L. 1980, Astr. and Ap., 85, 80.

Gehren, T., Fried, J., Wehinger, P. A., and Wyckoff, S. 1984, Ap. J., 278, 11.

Katgert, P. 1976, Astr. and Ap., 49, 221.

Koo, D. C., and Kron, R. G. 1982, Astr. and Ap., 105, 107.

LaViolette, P. A. 1986, Ap. J., 301, 544.

Machalski, J. 1978, Astr. and Ap., 65, 157.

Marshall, H. L., Avni, Y., Braccesi, A., Huchra, J. P., Tananbaum, H., Zamorani, G., and Zitelli, Z. 1984, Ap. J., 283, 50.

Schmidt, M., and Green, R. F., 1983, Ap. J., 269, 352.

Segal, I. E. 1976, Mathematical Cosmology and Extragalactic Astronomy (Academic Press: New York)

Segal, I. E., Loncaric, J., and Segal, W. 1980, Ap.J., 239, 38.

Segal, I. E., and Nicoll, J. F. 1986, Ap. J., 300, 224.

Wall, J. V., Pearson, T. J., and Longair, M. S. 1980, MNRAS, 193, 683.

Yee, H. C. 1983, Ap. J., 272, 473.

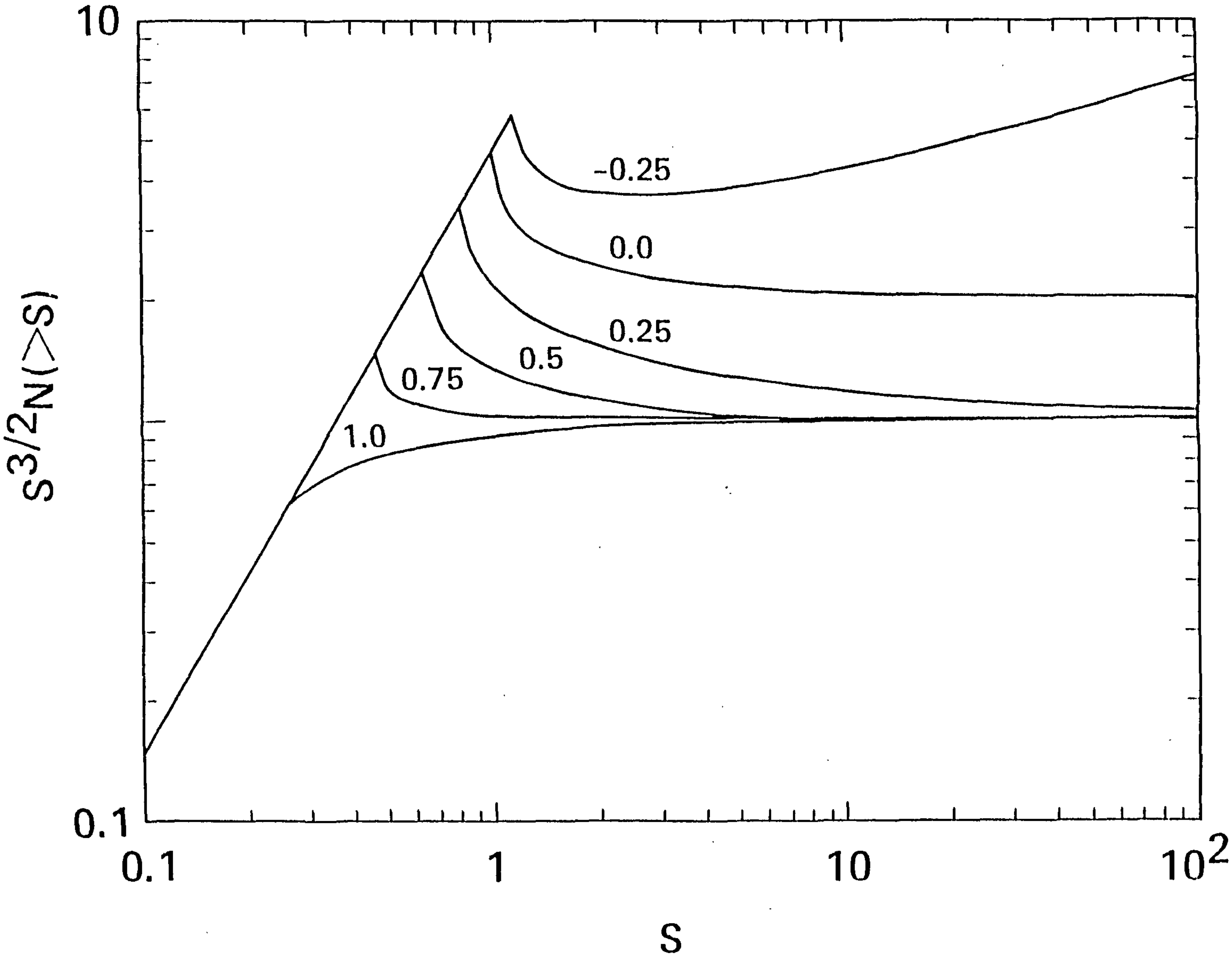

FIGURE 1: Chronometric model number counts (divided by a Euclidean law) for α = 1, 0.75, 0.5, 0.25, 0, and -0.25.

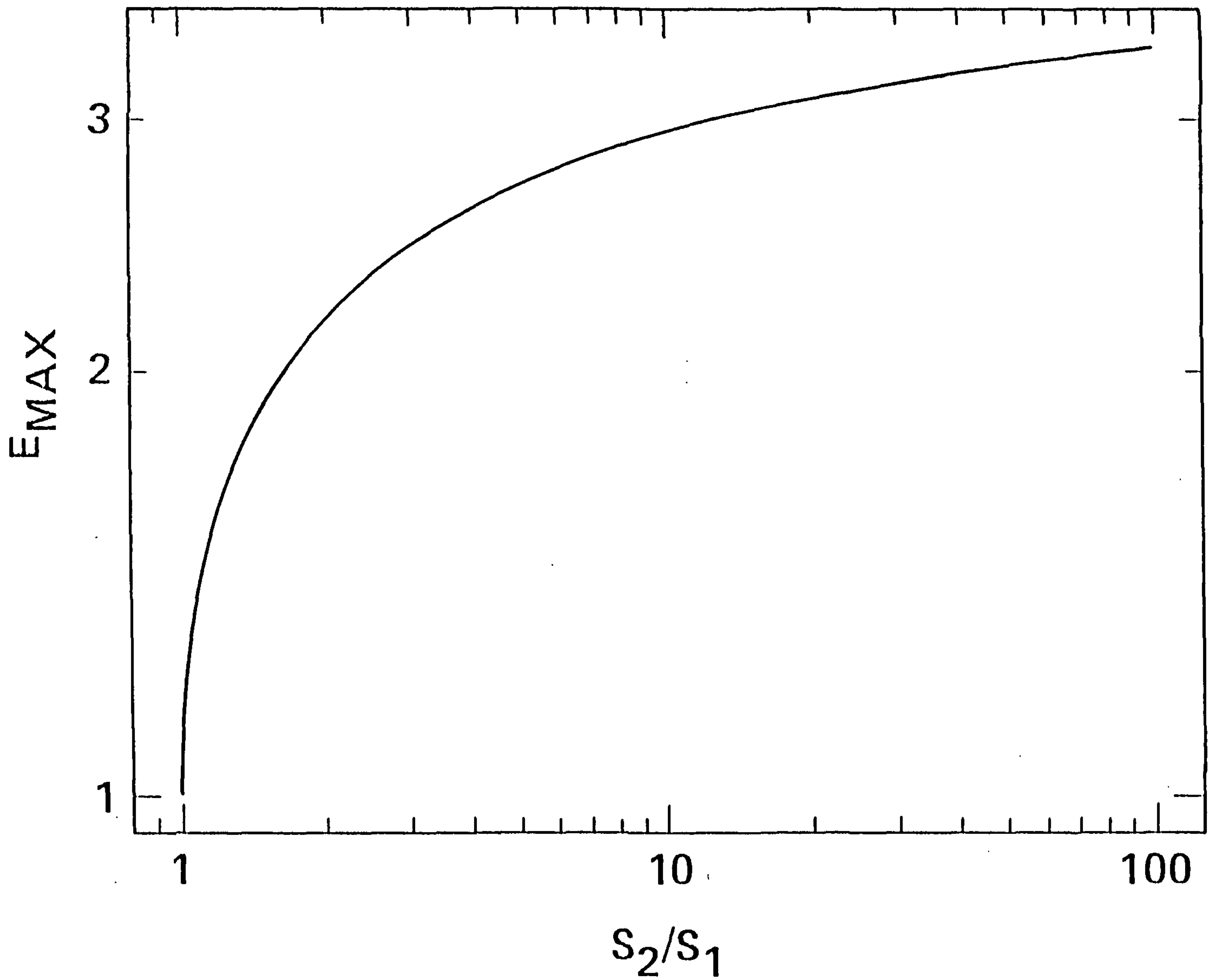

FIGURE 2: Maximum excess over Euclidean counts versus flux range in the chronometric model.

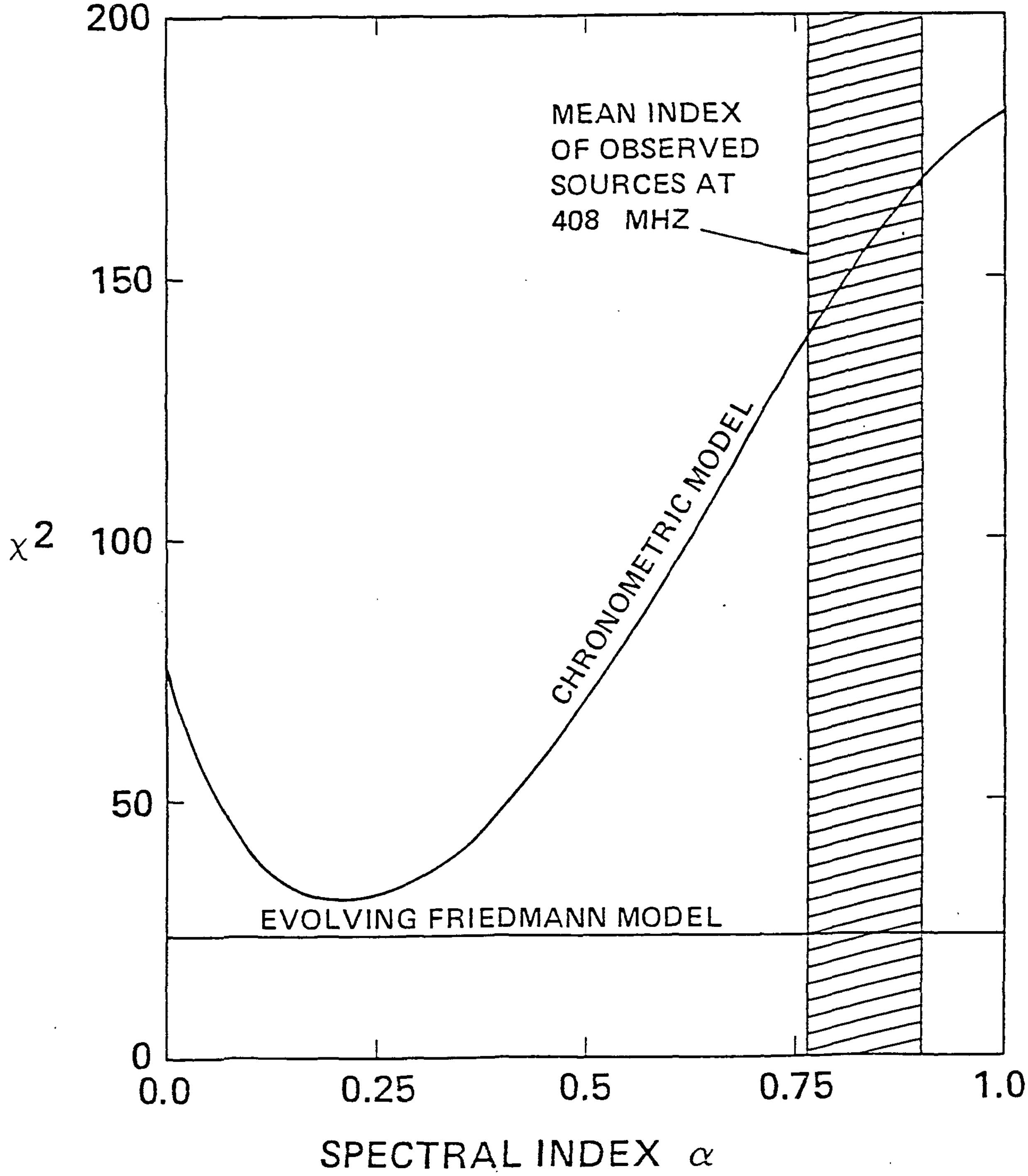

FIGURE 3: Goodness of fit χ^2 vs spectral index α for chronometric models of the 408 MHz radio source counts. The mean spectral index of 408 MHz sources is marked. The Wall et al. evolving Friedmann model is also shown.

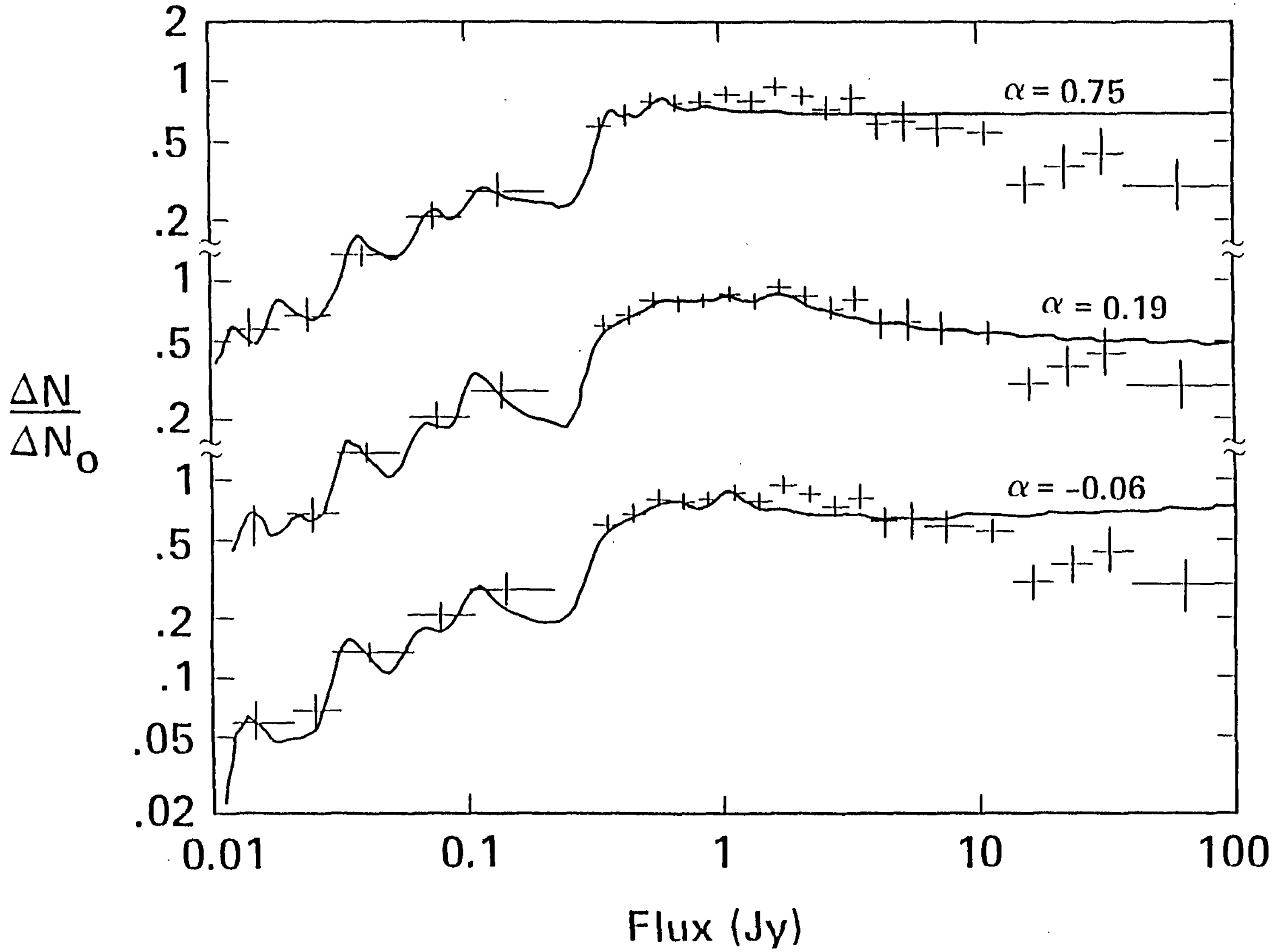

FIGURE 4: Chronometric model fits compared with 408 MHz source counts. Top: $\alpha = 0.75$, $\chi^2 = 136$. Middle: $\alpha = 0.19$, $\chi^2 = 30$. Bottom: $\alpha = -0.06$, $\chi^2 = 124$. Models and data have been normalized to a Euclidean N(S) law, $N_o = 1200\ S^{-1.5}$.

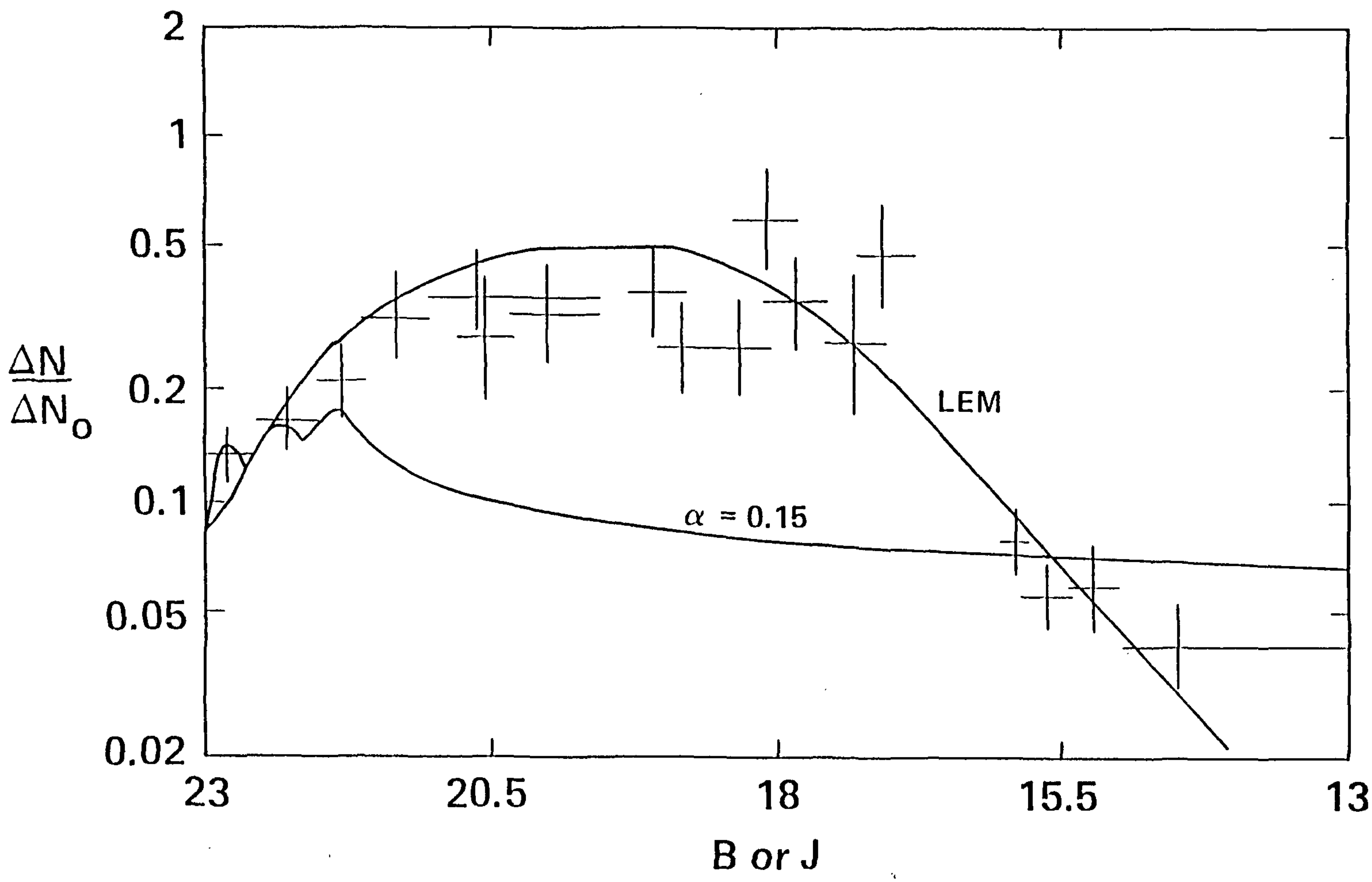

FIGURE 5: Model fits compared to optical quasar counts. LEM: luminosity evolution model of Braccesi et al.; α = 0.15: best fitting chronometric model.

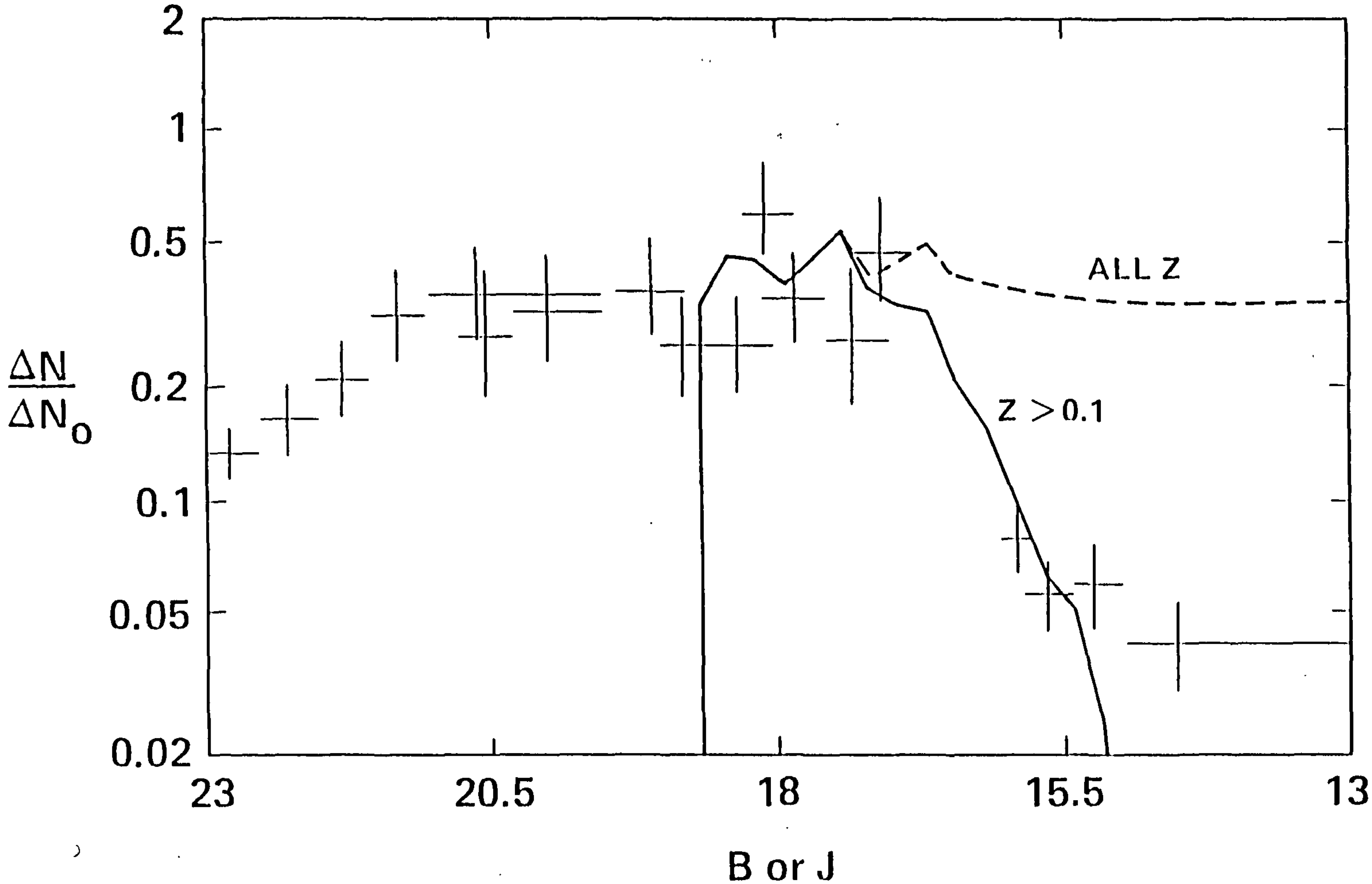

FIGURE 6: Segal and Nicoll model compared to quasar counts: with redshift restricted to z > 0.1 (solid curve), and the same model with no redshift restriction (dashed curve).

THE R/IR EVOLUTION IN GALAXIES - EFFECT OF THE STARS ON THE AGB

Arati Chokshi and Edward L. Wright

Dept. of Astronomy, University of California, Los Angeles, CA 90024

ABSTRACT

The effect of including the AGB population in a spectral synthesis model of galaxy evolution is examined. Stars on the AGB are luminous enough and also evolve rapidly enough to affect red and infrared evolution in galaxies. The validity of using infrared colors as distance indicators to galaxies is then investigated in detail.

INTRODUCTION

Over the years ample evidence has gathered indicating that galaxies evolve (eg., Djorgovski and Spinrad 1985; Bruzual and Spinrad 1981). One of the primary motivations for studying galaxy evolution has been that galaxies and galaxy distributions are principal probes for the study of the nature of the Cosmos and, in principle, can be used to derive values for cosmologically interesting parameters, such as the deceleration parameter q_0. Systematic effects of galaxy evolution must first be fully understood, however before one can successfully use giant elliptical galaxies at cosmologically interesting look back times, to probe the expansion of the universe. Also, the effects of galaxy evolution could completely mislead the efforts directed in estimating a value of q_0 via the standard route of Hubble plots (Tinsley and Gunn 1976). Evolution makes the distant younger galaxies brighter. This effect must be decoupled from a similar effect of a positive value for q_0

or Ω_0 (the ratio of the present density in the universe to critical density), which provides a smaller comoving volume within a specified z and therefore makes the galaxies appear brighter [because they are actually closer] than for the $q_0 = 0$ case.

One of the methods that has frequently been used to study the evolution of stellar population in galaxies is that of evolutionary spectral synthesis pioneered by Tinsley (1972) and elaborately modelled by Bruzual (1981). The input physics these models require are analytical expressions for the IMF and SFR, and the evolutionary tracks for stars on the HR diagram. Galaxy evolution [luminosity and spectral evolution] is then governed by the evolution of stars on the HR diagram. A general description of galaxy evolution may be given as follows: When a galaxy is young, its light is dominated by hot, bright, blue stars on the main sequence. Evolution causes an increased population of stars on the giant branch and it is the light from these red giants that dominates the red and infrared colors of galaxies. It is also apparent that evolutionary effects depend on the galaxy type in question i.e. different types of galaxies undergo star-formation at different rates and are therefore characterised by different spectral energy distributions at a given epoch. Further the effects of galaxy evolution are most pronounced in the near UV and visible and it is generally accepted that they do not effect the infrared colors significantly. Spectral energy distributions in the infrared are similar for all galaxy types since it comes the K and M giants. For these reasons, infrared colors are regarded as good distance indicators for galaxies. One point that has generally been overlooked is the rapid evolution of the bright red giants on the AGB, which could significantly affect the R/IR colors of galaxies in the course of their evolution. A detailed inclusion of the stars on the AGB into the spectral synthesis model of galaxy evolution has not been feasible to date simply because of a lack of reliable evolutionary tracks in this phase of stellar evolution. In this paper, we attempt to include the AGB light, in an evolutionary correct fashion, into the models of galaxy evolution developed by Bruzual(1981). We do this mainly from the energy output considerations, using a procedure developed by Renzini (1981), instead of attempting to extend the evolutionary sequence for stars on the HR diagram.

Section II details the procedures involved. Section III contains the results and analysis. The question of IR colors as distance indicators is re-examined. Section IV outlines a summary.

II. PROCEDURE

We make use of Renzini's model (1981) for a Simple Stellar Population (SSP), which is defined as a coeval population of single stars of the same initial chemical composition (assumed solar). The model enables a calculation of the fractional contributions of the various phases of stellar evolution to the total integrated light of a SSP. Renzini points out that the critical factors that determine these fractions are not the individual luminosities of stars in the various PMS (Post Main-Sequence) phases, nor the individual durations of the phases, but only the total amount of energy liberated, or the "fuel" burnt by a star in a particular phase of evolution. Thus, one does not need to consider the time evolution through the various PMS phases. Also, since the total time spent as a PMS star is small compared to the lifetime of a star, one can assume that the initial masses of stars in the various PMS phases are equal to the main sequence turnoff mass in a SSP. It is important to notice that the contribution of the AGB light in Renzini's SSP comes in very sharply and also very strongly at a definite age and it very soon dominates the integrated brightness of the SSP [see Fig(1) of Renzini and Buzzoni(1983)].

We adapted this method to calculate the energy($=E_{AGB}$) liberated by stars of various masses in their AGB phase. We used the calculations for the PMS contributions to the total light [see Fig(1) of Renzini and Buzzoni(1983)], calculated the flux of stars passing through the PMS($=b$) and the total bolometric luminosity of a SSP($=L_{tot}$) as a function of time. The stellar energy contribution in any PMS phase (for example the AGB phase) as a function of the age of the SSP, or its turnoff mass was then derived as follows: The percentage contribution in the AGB phase($=$AGB%) for a given turnoff mass is

$$\mathrm{AGB\%} = 100bE_{AGB}/L_{tot}$$

or,

$$E_{AGB} = \mathrm{AGB\%}\ L_{tot}/(100b) \qquad \text{------------}(1)$$

Fig (1) shows the energy contributions in the various phases as a function of stellar mass. Notice that the AGB contribution is important for stars between 1 to 8 $M_{\odot}$.

We incorporated the AGB contributions into Bruzual's (1981) galaxy evolution models as follows: Evolutionary tracks for stars in the HR-diagram that Bruzual used went only up to the Red Giant Tip(RGT) or the core helium burning phase in stars. Following Tinsley (1978), Bruzual attempted to remove the deficiency of stars on the AGB by semi-empirically extending the lifetimes that stars spent at the end of their red giant branch evolution, so that the synthetic red and infrared colors matched the R/IR observations of the E/S0 galaxies by Frogel et.al.(1978). This procedure, although adequate in describing the R/IR light in early type galaxies at the present epoch could not be relied on to produce an evolutionary correct sequence of IR contributions at earlier epochs.

We modified the evolutionary steps along the giant branch in Bruzual's program as follows: We removed the empirical correction for the AGB stars such that the evolutionary tracks corresponded to the original giant branch of Tinsley and Gunn (1976). We next added on the AGB energy contributions for stars of various masses, at their respective RGTs, such that a star remained at the RGT [i.e. at the same luminosity and temperature] for as long as was required to liberate the right amount of energy, as derived from Renzini's model. We believed it justifiable to use the same temperature as at the RGT, since the tracks on the AGB follow roughly the Hayashi tracks, but also because this was a reasonable approximation in the absence of detailed track information. Also, since the evolutionary time spent by a star on the AGB is short, a non-evolving luminosity was again a reasonable approximation as long as the energy output requirements were fulfilled.

A point that we have considered in the present work was the effect that a separate population of carbon stars might have on the infrared colors of galaxies. Some stars on the AGB go through a short phase of being carbon stars(Renzini, Voli 1982). Their spectra are characterised, amongst other things, by an ultraviolet depression which makes their visual colors considerably redder than those of normal red giants. However their effective temperatures are not very different from K and M giants with similar spectra at red wavelengths (Gunn, Stryker 1983 -figs 2p and 2s). Also Renzini and Voli (1982) estimate that only about 10% to 20% of the AGB stars go through the carbon star phase. For all these reasons, we believe, that carbon stars cannot make significant differences to the IR colors of galaxies and therefore all AGB stars used in model calculations are O-rich. The effect of including such a population would be much more pronounced in the B-V color index and this has been considered by Wyse (1985).

For a consistency check, we also used Renzini's model of an SSP to build up a synthetic galaxy. We combined a large number of SSP's such that they mimicked the overall shape of an exponential star-formation rate (SFR) that described a Bruzual model galaxy. We call this a Simple Galaxy (SG). In all cases we used Bruzual's parameterisation of an exponential SFR by μ, which represents the fraction of the total galaxy mass that is converted into stars in 1 Gyr. i.e.,

$$\mu = 1 - \exp\,(-1\ \mathrm{Gyr}/\tau) \qquad \text{----------(2)}$$

where τ is the characteristic time scale for galaxy evolution. The value of μ that we generally use is $\mu = 0.7$. Such a model would imitate an early type galaxy with a high SFR at early epochs and very little residual star formation at the present epoch. Each of the SSP making up our SG was described by Miller and Scalo's (1979) four-segment power law IMF, which is

$$\mathrm{IMF} = A_i M^{-(1+x)} \qquad \text{----------(3)}$$

where,

$$x = 0.25 \text{ for } 0.08 \leq M < 1.01$$
$$x = 1.01 \text{ for } 1.01 \leq M < 1.95$$
$$x = 1.30 \text{ for } 1.95 \leq M < 8.37$$
$$x = 2.30 \text{ for } 8.37 \leq M < 25.0 \qquad \text{----------(4)}$$

where the normalisation factors A_i make the IMF continuous . Then to derive the PMS contributions from this SG we just added up the contributions of the various PMS phases for all the SSPs making up the galaxy. We could now make a direct comparison between these results and the corrected Bruzual's model.

III RESULTS AND ANALYSES

The results that we derived for the fractional PMS contribution from a model galaxy are shown in Fig 2. Here, the fractional PMS bolometric light is plotted as a function of the age of the galaxy, for Bruzual's original model, for the corrected version of Bruzual's model and for a SG. One notices that the corrections to Bruzual's model produces results that appear to be consistent with what we derive from Renzini's model, at later stages of evolution. Also, at younger galaxy ages, we notice that there is an agreement between our model, Bruzual's model and a SG only if we were to ignore the Horizontal Branch (HB) stars contributions in Renzini's model. This implies that Bruzual's models are deficient in HB light at early epochs of galaxy evolution, although the residual star formation in a μ-model at later times are adequate in providing an empirical fit between the observed and synthesised spectra in the UV. Note that we have made no attempt to correct for a HB population in Bruzual's model and this explains the similarity of the two results at earlier times. A better overall fit would require a careful consideration of the HB population especially at younger galaxy ages. Fig 3 is a plot of the ratio of light from various PMS phases to the total PMS light in a SSG, as a function of age. Notice the importance of HB population at early epochs. The figure also illustrates the strong dominance of the AGB light at a fixed epoch after the galaxy formation.

A very interesting feature of our corrections to Bruzual's model is its effect on the spectral evolution of the model galaxy. Fig 4 is plot of galaxy spectra [Log F_ν -Log λ] as a function of galaxy age. One notices a "hump" appear at the red end of the spectra at a galaxy age of about 0.2 Gyr. This represents the sudden appearance of stars on the AGB. Such a feature is reproduced in our infrared color evolution plots showing (V-K), (J-H) and (B-V) plotted as a function of galaxy age [FIG 5]. No significant differences are noticed in the evolution of (B-V) color index. Table(1) lists the various color indices as a function of galaxy age. Model parameters are specified.

We note in the infrared color evolution plots that at galaxy ages larger than about a billion years the infrared colors flatten into a plateau i.e. there is no significant IR evolution up to rather large z in the galaxy rest frame. However, if the epoch of galaxy formation is sufficiently recent, as considered by some authors (Tinsley 1977) then one will begin seeing the effects of evolution at fairly short lookback times and, interestingly, if one is examining the red/infrared colors, the tendency will be for the galaxies to first appear redder at younger ages and then get bluer. However such a trend will not be apparent in the visual or blue color indices. Table II lists the redshifts up to which IR evolution,in the galaxy rest frame, can be regarded as in-significant. This is shown as a function of H_o and Ω_o. From Figs 5(a,b) we notice that there is very little IR color evolution beyond a galaxy age of $t \simeq 3$ Gyrs (or, $\log(\text{age}) \simeq 9.5$). Assuming the limiting case for the epoch of galaxy formation at $z = \infty$, and values for H_o and Ω_o, enables a calculation of the look back time (Δt) to the epoch when galaxy evolution becomes significant. This is then converted into redshift via.,

$$z = [1-H_o\ \Delta t]^{-1} - 1 \qquad \text{for } q_o = 0 \text{ or } \Omega_o = 0.$$

$$z = [1-1.5\ H_o\ \Delta t]^{-(2/3)} - 1 \qquad \text{for } q_o = 1/2 \text{ or } \Omega_o = 1 \quad \text{---------(5)}$$

One interesting point that we noticed in our calculations was that even if we repeated the entire procedure for a very slowly evolving galaxy [eg., μ=0.01] i.e., a galaxy with significant amount of current star forming activity or a late type system, the "hump" feature is reproduced both in the spectra [Fig 4] and in the IR color evolution plots (see Figs 5 and Table 1) at the same epoch after galaxy formation as in early type systems. Also it appears that the late type systems retain a considerable amount of their AGB populations all through their evolving lifetimes. This is evidenced in their red R/IR color indices at late times even though they are much bluer in B-V than the early type systems. It thus appears that the infrared evolution in galaxies is almost independent of the SFR in galaxies.

A very exciting possibility then seems to be that since this "hump" in the IR colors and spectra seems to appear at such a well defined age after the galaxy formation and is irrespective of the galaxy type, one could in principle, constrain the epoch of galaxy formation based upon observed red evolution of the IR colors. This is certainly feasible if the epoch of galaxy formation is sufficiently recent. A similar suggestion that color evolution may be used to constrain the epoch of galaxy formation has been considered by Wyse (1985).

Two factors that influence the observed fluxes and/or colors from a galaxy are the redshift of the galaxy continuum i.e., the K-correction and the galaxy spectral energy distribution (s.e.d) at that redshift i.e. the evolutionary correction. Table III lists the observed IR color, defined as the ratio of the observed fluxes at 2 and 4 microns, from model galaxies with three different SFRs given by μ = 0.01, 0.7, 0.9 respectively and from a non-evolving galaxy, where only the effect of redshifting the z = 0 continuum for a μ = 0.7 galaxy has been considered. Tabulations include two different cosmologies (Ω_0=0 and

Ω_o=1) for H_o=50 at a galaxy age of 12 Gyr and two different galaxy ages T_g= 19 Gyr and 15 Gyr for cosmological parameters H_o=50 and Ω_o=0 respectively. The effect of using different Ω_o on the measured fluxes or observed colors is as follows: A given time t measured from any event up till now, corresponds to a larger redshift in a Ω=1 universe than in the case of an empty or Ω=0 universe, or in other words a redshift of galaxy formation z_{form} corresponds to a more recent event in a Ω=1 model. This means that one tends to see younger galaxies and stronger evolutionary effects in models with larger Ω. most extreme case that we consider (T_g = 12Gyr and Ω_o = 0) one essentially reaches the epoch of galaxy formation at z ≈1.5. Obviously, such a case is be ruled out by the observations of galaxies at redshifts of up to 1.84 (Djorgovski, Spinrad 1984), if one makes the simplifying assumption of a single epoch of all galaxy formation. The latter assumption however may not be viable.

Figs 6 a-d are plots of the ratio of 2 to 4 micron monochromatic fluxes vs. redshift for the four cases discussed above. One notices that for large galaxy ages (T_g=19 Gyr) there is of the order of a magnitude difference in colors between the evolving and non-evolving galaxies at a redshift of 5. The most striking feature about all these plots is that beyond a redshift of z ≈ 1 the observed colors seem to flatten out or get bluer implying that the evolutionary effects compensate and even dominate the effect K-correction at these IR wavelengths and are independant of the galaxy type i.e., the SFR. This would limit the use of IR-colors as distance indicators to fairly nearby galaxies. In principle one could apply evolutionary correction to galaxy fluxes, especially since the affect of varying the SFR seems secondary. The primary factors neccessary before this can be done are the constraints on galaxy age T_g and the cosmological parameters H_o and Ω_o. However, although it is possible to estimate the galaxy age observationally, as discussed above, the determination of H_0 and Ω_0 present a much more formidable task especially since one does not have a readily available method of distance determination for distant galaxies.

Finally, Figs 7 a-b show a comparison between our predicted H-K color index as a function of redshift with the results of near infrared photometry on giant elliptical galaxies with known redshifts (Eisenhardt, Lebofsky,1986). The data are compared with model predictions based on both non-evolving and evolving spectral energy distributions for each of the following two cases: (1) t_g= 9 gyr, H_0= 100, q_0= 0 and (2) t_g=16 gyr, H_0= 50, q_0=0. SFR parameter μ = 0.7 is used to characterise the star formation activity in elliptical galaxies. It should be noted that the real data are based on the observations of both optically selected and radio selected galaxies. However the authors find no significant evidence for differences between these two galaxy types based on the properties of their infrared colors.

One observes that the model predictions do follow the basic trend of the data quite well, although one must be cautioned against relying on models to reproduce either the detailed characteristics or make accurate description of color evolution in galaxies. This is mainly due to the fact that the model s.e.ds of galaxies are only coarsely described at the near infrared wavelengths and any improved treatment would require an inclusion of the detailed spectral characteristics of cool stars that dominate the longer wavelength regime. At this point it is encouraging that Bruzual's models do roughly reproduce the visual (Bruzual 1981) and the infrared colors observed in the nearby galaxies as well as show the same trend as the data as with increasing redshifts. A final point that should be made is that the data only extend up to a redshift of 1.2 at which point the different models are barely beginning to show the evolutionary effects due to the AGB stars that we have included. More observations of this kind that extend to larger redshifts are neccessary before one can understand and/or quantify the evolutionary effects in galaxies.

IV. CONCLUSION

We conclude that (1) a population of AGB stars can make significant changes to the evolution of galaxies in the R/IR colors. In particular galaxies at a higher z would appear to get redder in their rest frame. However, such effects of evolution would be observable only if the epoch of galaxy formation were sufficiently recent. One could, in principle, constrain the epoch of galaxy formation by observing the evolution of infrared colors. (2) Late type systems seem to have a considerable amount of red and infrared stellar light i.e., their colors and luminosities are governed by a very wide variety of stellar population. (3) Addition of the AGB population produces colors that are still consistent with the observed range for E/S0 galaxies since its effect will not be apparent till about a redshift of 1. (4) Near IR colors can be used as distance indicators up to $z < 1$, but at higher redshifts spectral evolution causes a wide range in colors.

Acknowledgements: The authors would like to thank Gustavo Bruzual for the use of his computer programs that modelled spectral energy distributions in galaxies. A. Chokshi is grateful to S. Djorgovski for his help in the use of Bruzual's computer programs. This research was supported in part by the NASA grant# NAG2-315.

REFERENCES

1. Bruzual, A. G., 1981, Ph.D Thesis, University of California, Berkeley
2. Bruzual, A. G., Spinrad, H., 1981, The Universe at Ultraviolet Wavelengths : The First Two years of IUE, ed.- R. D. Chapman (NASA: Goddard Space Flight Center)
3. Djorgovski, S., Spinrad, H., 1985, preprint
4. Eisenhardt, P., Lebofsky, M., 1986, preprint
5. Frogel, J. A., Persson, S. E., Aaronson, M., Matthews, K., 1978, Ap.J., 220, 75
6. Gunn, J. E., Stryker, L. L., 1983, Ap.J. Supp., 52, 121
7. Miller, G. E., Scalo, J. M., 1979, Ap.J. Supp., 41, 513
8. Renzini, A., 1981, Ann. Phys. Fr., 6, 87
9. Renzini, A., Buzzoni, A., 1983, Mem. S. A. It., 54, 739
10. Renzini, A., Voli, M., 1981, Astr. Ap., 94, 175
11. Tinsley, B. M., 1972, Astr. Ap., 20, 383
12. Tinsley, B. M., 1977, Ap. J., 211, 621
13. Tinsley, B. M., 1978, Ap. J., 222, 14
14. Tinsley, B. M., Gunn, J. E., 1976, Ap. J., 203, 53
15. Wyse, R., 1985, pvt. communications

TABLE I

COLOR EVOLUTION IN MODEL GALAXIES (Rest Wavelengths)

	μ = 0.7 [old]			μ = 0.7			μ = 0.01		
AGE(Gyr)	V-K	J-H	B-V	V-K	J-H	B-V	V-K	J-H	B-V
0.01	-0.45	0.00	-0.21	-0.45	0.00	-0.21	-0.45	0.00	-0.21
0.05	1.37	0.58	-0.11	1.37	0.58	-0.12	1.35	0.57	-0.11
0.10	1.47	0.56	-0.03	1.60	0.59	-0.01	1.58	0.59	-0.02
0.20	1.96	0.67	0.02	3.62	0.89	0.05	3.57	0.88	0.04
0.30	2.16	0.64	0.22	3.31	0.84	0.23	3.32	0.84	0.20
0.40	2.07	0.62	0.24	3.15	0.81	0.29	3.19	0.82	0.25
0.75	1.76	0.55	0.21	2.93	0.78	0.32	3.02	0.79	0.29
1.00	1.74	0.51	0.21	2.73	0.75	0.30	2.89	0.78	0.28
2.00	2.20	0.61	0.39	2.86	0.75	0.45	2.87	0.76	0.36
3.00	3.05	0.76	0.60	3.67	0.84	0.63	3.22	0.80	0.44
4.00	3.13	0.76	0.68	3.72	0.84	0.69	3.29	0.81	0.47
5.00	3.28	0.77	0.77	3.85	0.85	0.79	3.35	0.81	0.50
6.00	3.25	0.76	0.81	3.80	0.84	0.82	3.38	0.81	0.52
7.00	3.23	0.76	0.84	3.72	0.83	0.85	3.39	0.81	0.54

TABLE I [continued]

	μ=0.7 [old]			μ=0.7			μ=0.01		
AGE(Gyr)	V-K	J-H	B-V	V-K	J-H	B-V	V-K	J-H	B-V
8.00	3.28	0.76	0.87	3.76	0.83	0.88	3.41	0.81	0.55
9.00	3.23	0.76	0.87	3.70	0.82	0.88	3.42	0.81	0.57
10.00	3.24	0.76	0.88	3.69	0.82	0.89	3.43	0.81	0.58
11.00	3.26	0.76	0.90	3.70	0.82	0.90	3.43	0.81	0.59
12.00	3.27	0.76	0.91	3.71	0.82	0.92	3.44	0.81	0.60
13.00	3.30	0.76	0.93	3.70	0.82	0.93	3.45	0.81	0.61
14.00	3.31	0.76	0.94	3.66	0.81	0.94	3.45	0.81	0.61
15.00	3.34	0.76	0.95	3.67	0.81	0.95	3.45	0.81	0.62
16.00	3.34	0.76	0.96	3.63	0.81	0.97	3.45	0.81	0.63
17.00	3.35	0.76	0.97	3.62	0.80	0.97	3.46	0.81	0.63
18.00	3.35	0.76	0.97	3.62	0.80	0.98	3.46	0.81	0.64
19.00	3.32	0.76	0.97	3.55	0.79	0.98	3.46	0.81	0.64

TABLE II

Cosmology	Age (To)	To - t*	z
H_o= 100			
Ω_o= 0	9.78 10^9	6.78	2.26
Ω_o= 1	6.55 10^9	3.55	0.69
H_o= 75			
Ω_o= 0	13.04 10^9	10.04	3.34
Ω_o= 1	8.74 10^9	5.74	1.05
H_o=50			
Ω_o= 0	19.56	16.56	5.52
Ω_o= 1	14.11	10.11	1.71

* Note: t is the age of the galaxy up to which the effects of evolution are pronounced. t= $3x10^9$ years [see Figs 4]

TABLE IIIa

OBSERVED IR (2-4)MICRON COLOR FOR MODEL GALAXIES

T_g = 12.0, z(formation)=1.58, H_o=50, Ω_o=0.

Age(Gyr)	z	$\lambda_e[2]^*$	$\lambda_e[4]$	Log [Flux (2µm) / Flux (4µm)]			
				µ= 0.01	0.7	0.9	0.7 [NE]
0.40	1.457	8139.06	16278.12	0.0334	0.0569	0.0792	0.0294
1.50	1.159	9263.80	18527.61	0.2553	0.3501	0.4216	0.0899
3.00	0.852	10797.55	21595.09	0.3766	0.3263	0.3032	0.3502
4.00	0.692	11820.04	23640.08	0.4997	0.4814	0.4771	0.4928
5.00	0.557	12842.54	25685.07	0.5866	0.5821	0.5809	0.5855
6.00	0.442	13865.03	27730.06	0.6444	0.6415	0.6415	0.6435
7.00	0.343	14887.53	29775.05	0.7210	0.7177	0.7210	0.7193
8.00	0.257	15910.02	31820.04	0.8248	0.8235	0.8254	0.8254
9.00	0.181	16932.51	33865.03	0.9818	0.9805	0.9809	0.9823
10.00	0.114	17955.01	35910.02	1.0334	1.0294	1.0334	1.0334
11.00	0.054	18977.51	37955.01	1.0899	1.0864	1.0864	1.0899
12.00	0.000	20000.00	40000.00	1.1790	1.1790	1.1790	1.1790

Note: $\lambda_e[2]$ is the emission wavelength in angstroms at a given z for the flux $F\lambda$ to be observed at 2 µm.

TABLE III b

T_g = 12.0, z(formation)=4.38, H_o=50, Ω_o=1.

Age(Gyr)	z	$\lambda_e[2]$	$\lambda_e[4]$	Log [Flux (2μm) / Flux (4μm)]			
				μ= 0.01	0.7	0.9	0.7 [NE]
0.40	3.345	4603.45	9206.90	0.3909	0.3766	0.3636	0.0128
1.50	1.976	6720.45	13440.90	0.2227	0.3243	0.4014	-0.0458
3.00	1.184	9157.23	18314.46	0.1399	0.0531	0.0128	0.0899
4.00	0.885	10612.00	21224.00	0.3263	0.2718	0.2601	0.3054
5.00	0.670	11972.97	23945.93	0.5145	0.4969	0.4928	0.5092
6.00	0.508	13260.48	26520.95	0.6085	0.6053	0.6053	0.6075
7.00	0.380	14488.22	28976.43	0.6893	0.6857	0.6884	0.6875
8.00	0.277	15665.95	31331.90	0.7959	0.7945	0.7966	0.7966
9.00	0.190	16800.94	33601.89	0.9576	0.9566	0.9571	0.9581
10.00	0.117	17898.80	35797.61	1.0294	1.0294	1.0294	1.0294
11.00	0.055	18963.97	37927.93	1.0864	1.0864	1.0864	1.0864
12.00	0.000	20000.00	40000.00	1.1790	1.1790	1.1790	1.1790

TABLE IIIc

T_g = 15.0, z(formation)=3.6, H_0=50, Ω_0=0.

Age(Gyr)	z	λ_e[2]	λ_e[4]	Log [Flux (2μm) / Flux (4μm)]			
				μ= 0.01	0.7	0.9	0.7 [NE]
0.40	2.944	5071.58	10143.15	0.3201	0.3096	0.3054	0.0128
0.75	2.684	5429.45	10858.90	0.2529	0.2529	0.2601	0.0253
1.00	2.518	5685.07	11370.14	0.2504	0.2923	0.3304	0.0086
2.00	1.982	6707.57	13415.13	0.1818	0.1931	0.1732	-0.0223
3.00	1.587	7730.06	15460.12	0.0792	-0.0334	-0.0878	0.0334
5.00	1.046	9775.05	19550.10	0.1614	0.0792	0.0645	0.1664
8.00	0.557	12842.54	25685.07	0.5855	0.5832	0.5855	0.5855
11.00	0.257	15910.02	31820.04	0.8254	0.8241	0.8241	0.8241
12.00	0.181	16932.51	33865.03	0.9814	0.9823	0.9805	0.9795
13.00	0.114	17955.01	35910.02	1.0334	1.0334	1.0334	1.0294
14.00	0.054	18977.51	37955.01	1.0899	1.0864	1.0899	1.0864
15.00	0.000	20000.00	40000.00	1.1790	1.1761	1.1790	1.1761

TABLE IIId

T_g = 19.0, z(formation)=33.6, H_0=50, Ω_0=0

Age(Gyr)	z	$\lambda_e[2]$	$\lambda_e[4]$	Log [Flux (2μm) / Flux (4μm)] μ= 0.01	0.7	0.9	0.7[NE]
2.5	5.392	3128.84	6257.67	0.0086	−0.2240	−0.6274	−0.9031
3.0	4.494	3640.08	7280.16	−0.0186	−0.2534	−0.6345	−0.5817
5.0	2.518	5685.07	11370.14	0.1139	−0.0414	−0.9217	0.0453
7.0	1.587	7730.06	15460.12	0.0414	−0.0123	−0.9930	0.0828
9.0	1.046	9775.05	19550.10	0.1584	0.1335	0.1303	0.2014
11.0	0.692	11820.04	23640.08	0.4987	0.4914	.4886	0.5079
13.0	0.442	13865.03	27730.06	0.6444	0.6444	0.6436	0.6464
15.0	0.257	15910.02	31820.04	0.8267	0.8241	0.8267	0.8267
16.0	0.181	16932.51	33865.03	0.9823	0.9809	0.9814	0.9814
17.0	0.114	17955.01	35910.02	1.0334	1.0334	1.0334	1.0334
18.0	0.054	18977.51	37955.01	1.0899	1.0899	1.0864	1.0864
19.0	0.000	20000.00	40000.00	1.1790	1.1761	1.1761	1.1761

FIGURE CAPTIONS

Fig 1 : Energy contributions as a function of turnoff mass for stars in various Post Main Sequence (PMS) phases.

Fig 2 : Fraction of PMS to total bolometric light in a model galaxy as a function of galaxy age: a comparison between various model predictions

Fig 3 : Fraction of the total PMS light coming from various stellar evolutionary phases as a function of age of a model galaxy.

Fig 4 : Evolving spectral energy distribution for a model galaxy with $\mu = 0.7$.

Fig 5 : Color evolution in the galaxy rest frame (a) B-V (b) V-K (c) J-H

Fig 6 : IR [2-4 μm] color evolution as a function of redshift in the observer's frame for different choices of omega (Ω) and galaxy age t_g (a)$\Omega = 1$, $t_g = 12$ (b)$\Omega = 0$, $t_g = 12$ (c)$\Omega = 0$, $t_g = 15$ (d)$\Omega = 0$, $t_g = 19$ Gyrs.

Fig 7 : Comparison between model predictions for H-K color index as a function of redshift with observed data for giant elliptical galaxies. Filled squares represent optically selected galaxies and stars represent the radio selected galaxies. Observed data from Eisenhardt and Lebofsky(1986). (a) $H_o = 100$, $t_g = 7$ Gyr (b) $H_o = 50$, $t_g = 16$ Gyr

MAILING ADDRESSES:

Arati Chokshi

Mail Stop 245/6

NASA Ames Research Center

Moffett Field, CA 94035

Edward L. Wright

Dept. of Astronomy

UCLA

Los Angeles, CA 90024

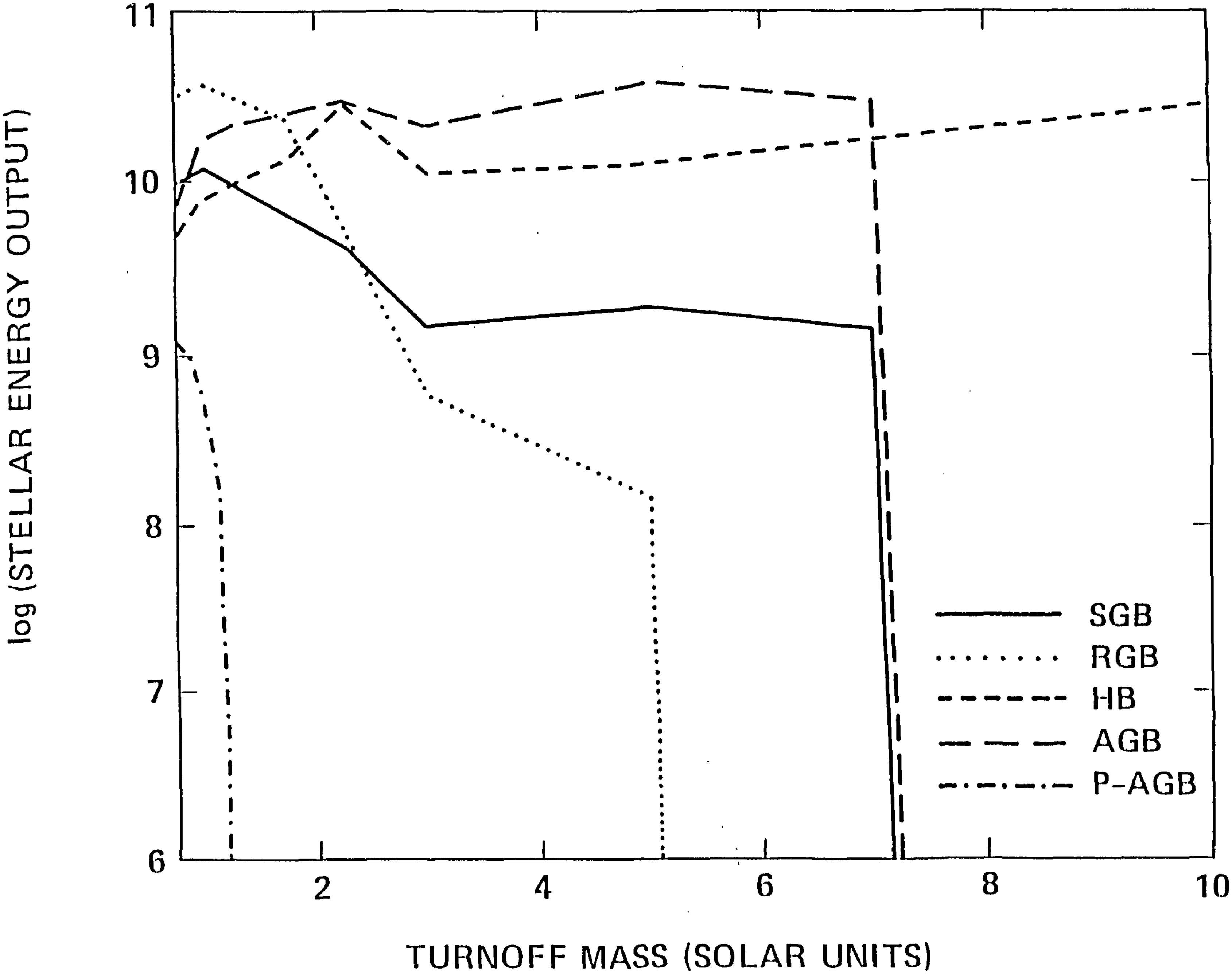

log (STELLAR ENERGY OUTPUT)
11
10
9
8
7
6
2
4
6
8
10
TURNOFF MASS (SOLAR UNITS)
SGB
RGB
HB
AGB
P-AGB

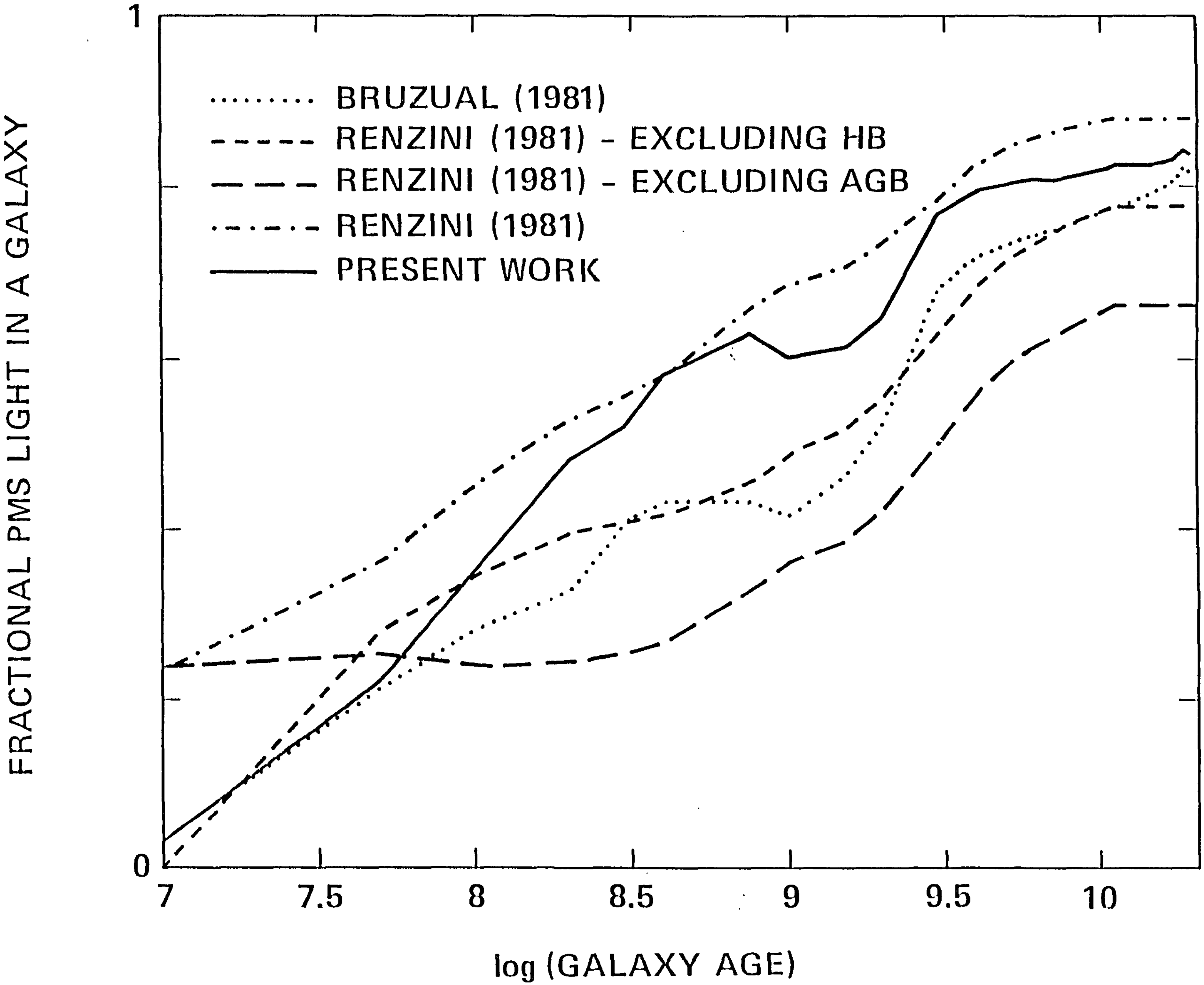

1
0
BRUZUAL (1981)
RENZINI (1981) - EXCLUDING HB
RENZINI (1981) - EXCLUDING AGB
RENZINI (1981)
PRESENT WORK
FRACTIONAL PMS LIGHT IN A GALAXY
7
7.5
8
8.5
9
9.5
10
log (GALAXY AGE)

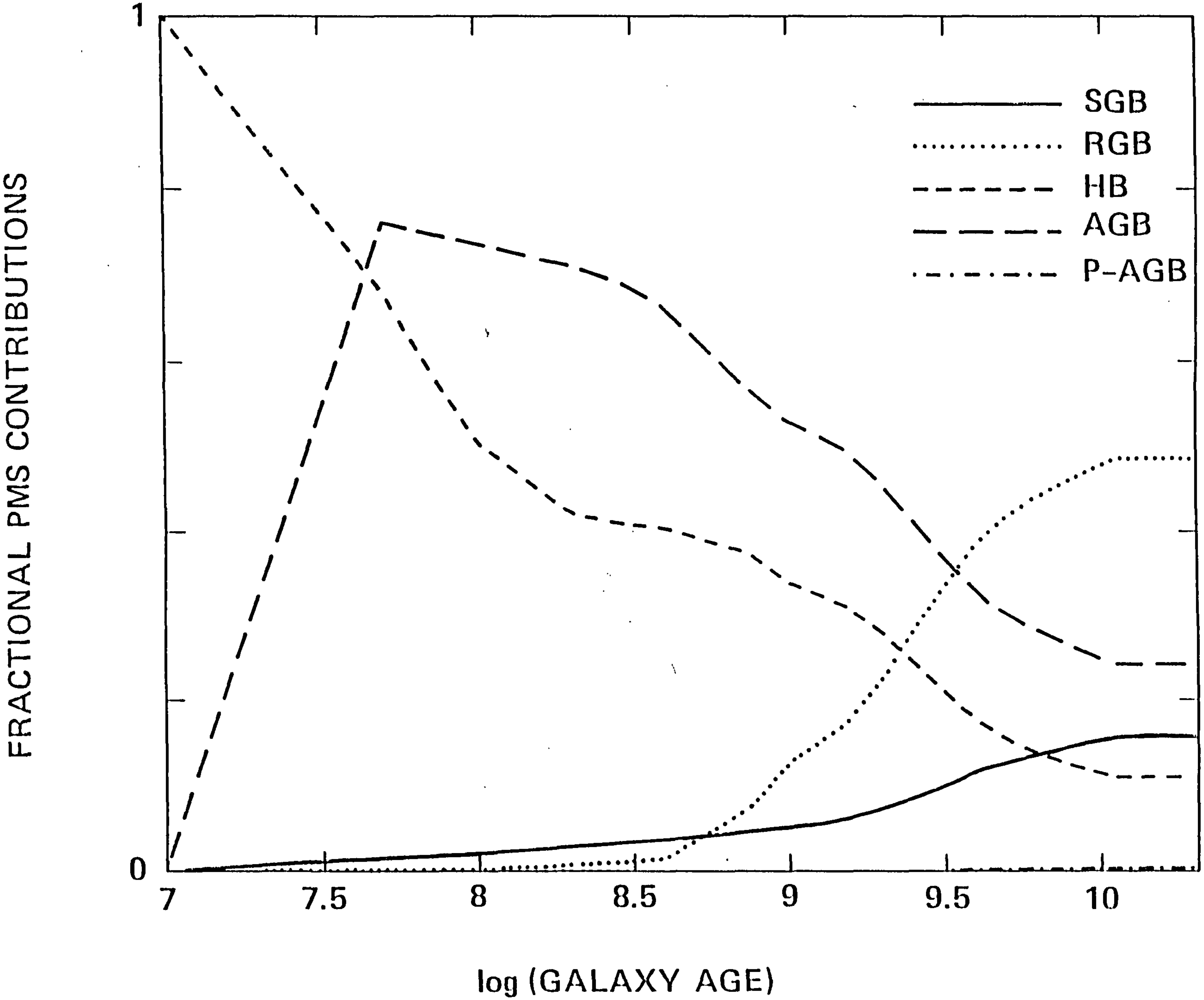

1
0
7
7.5
8
8.5
9
9.5
10
FRACTIONAL PMS CONTRIBUTIONS
log (GALAXY AGE)
SGB
RGB
HB
AGB
P-AGB

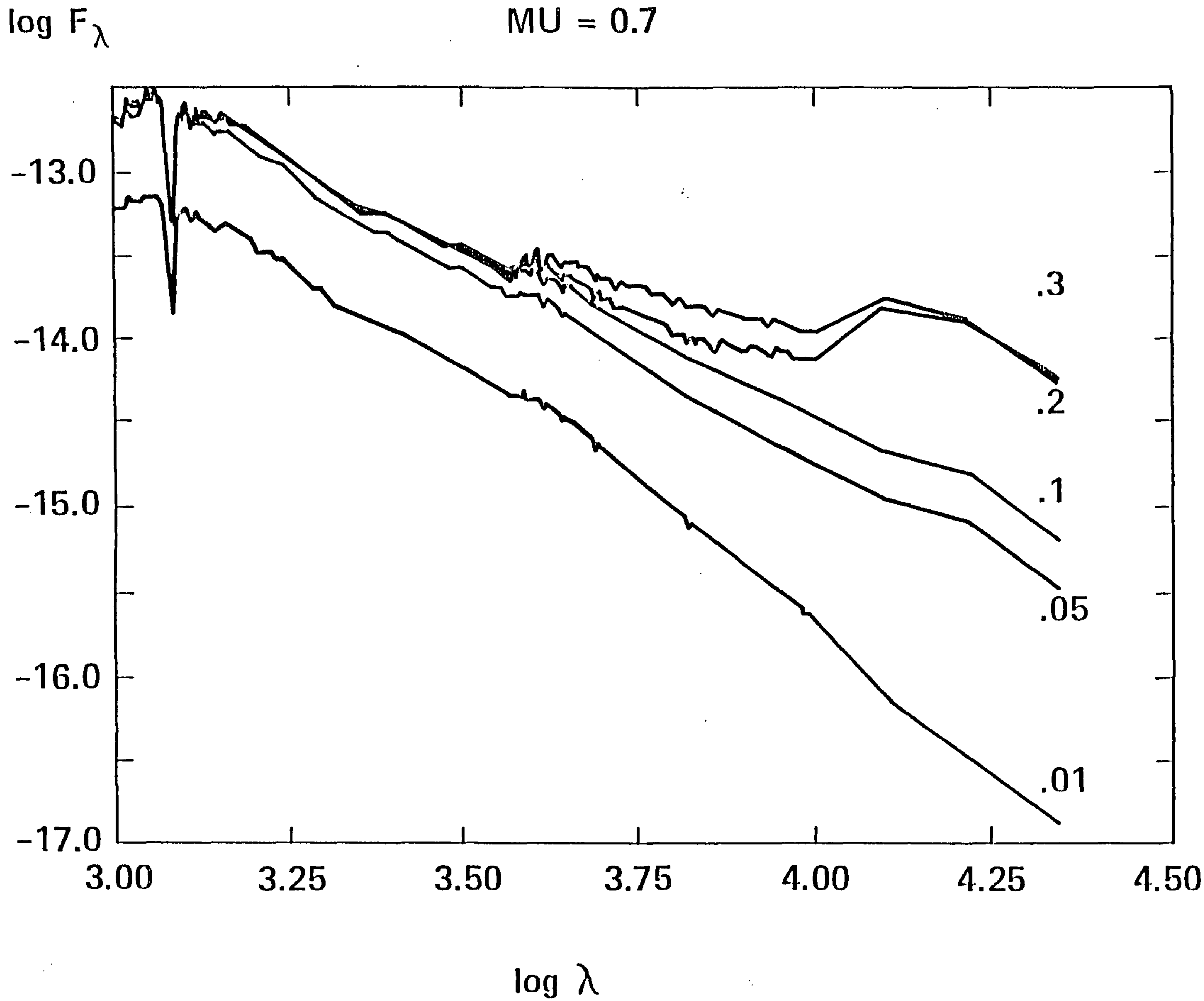

log F_λ
MU = 0.7
-13.0
-14.0
-15.0
-16.0
-17.0
.3
.2
.1
.05
.01
3.00
3.25
3.50
3.75
4.00
4.25
4.50
log λ

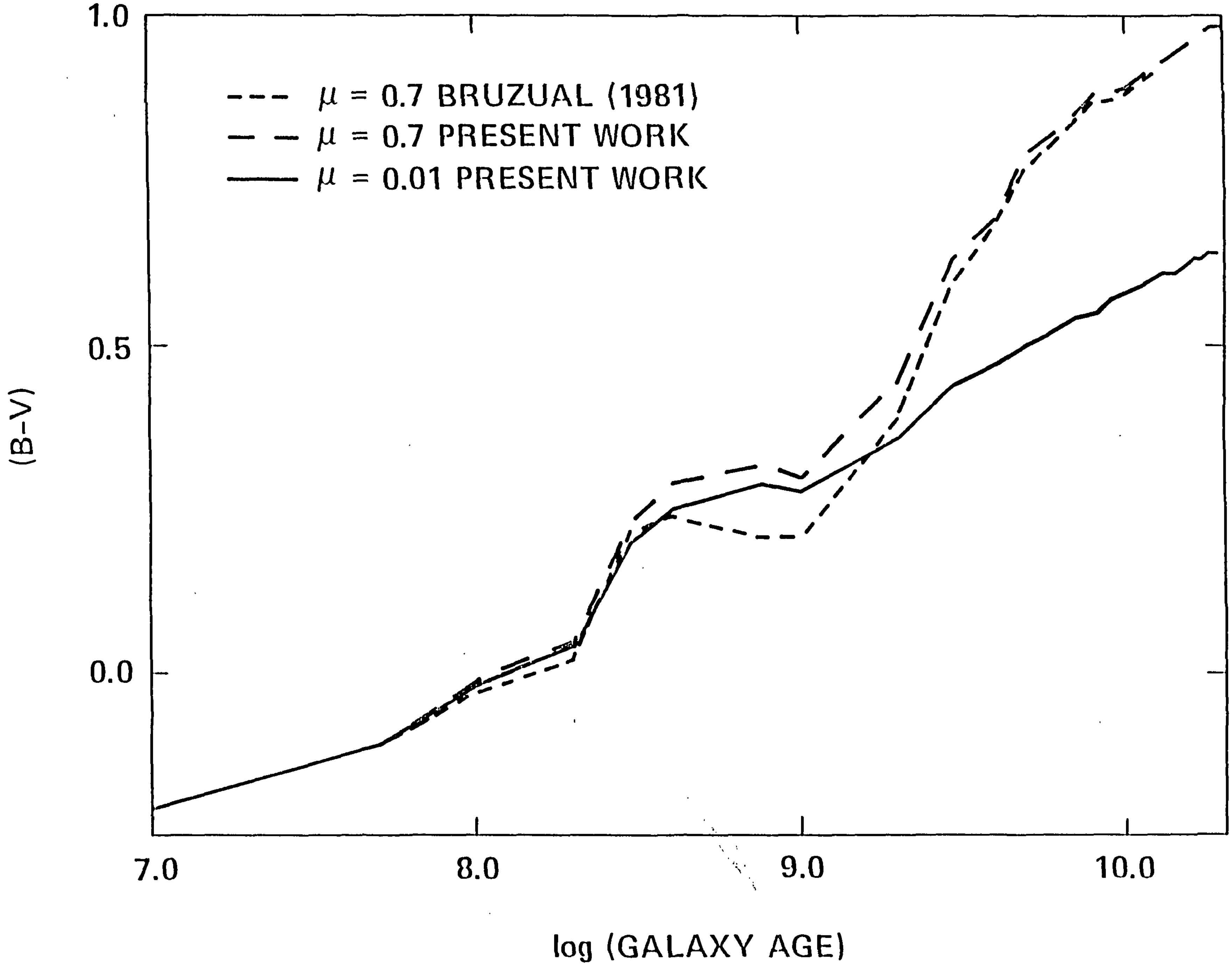

1.0
0.5
0.0
(B–V)
μ = 0.7 BRUZUAL (1981)
μ = 0.7 PRESENT WORK
μ = 0.01 PRESENT WORK
7.0
8.0
9.0
10.0
log (GALAXY AGE)

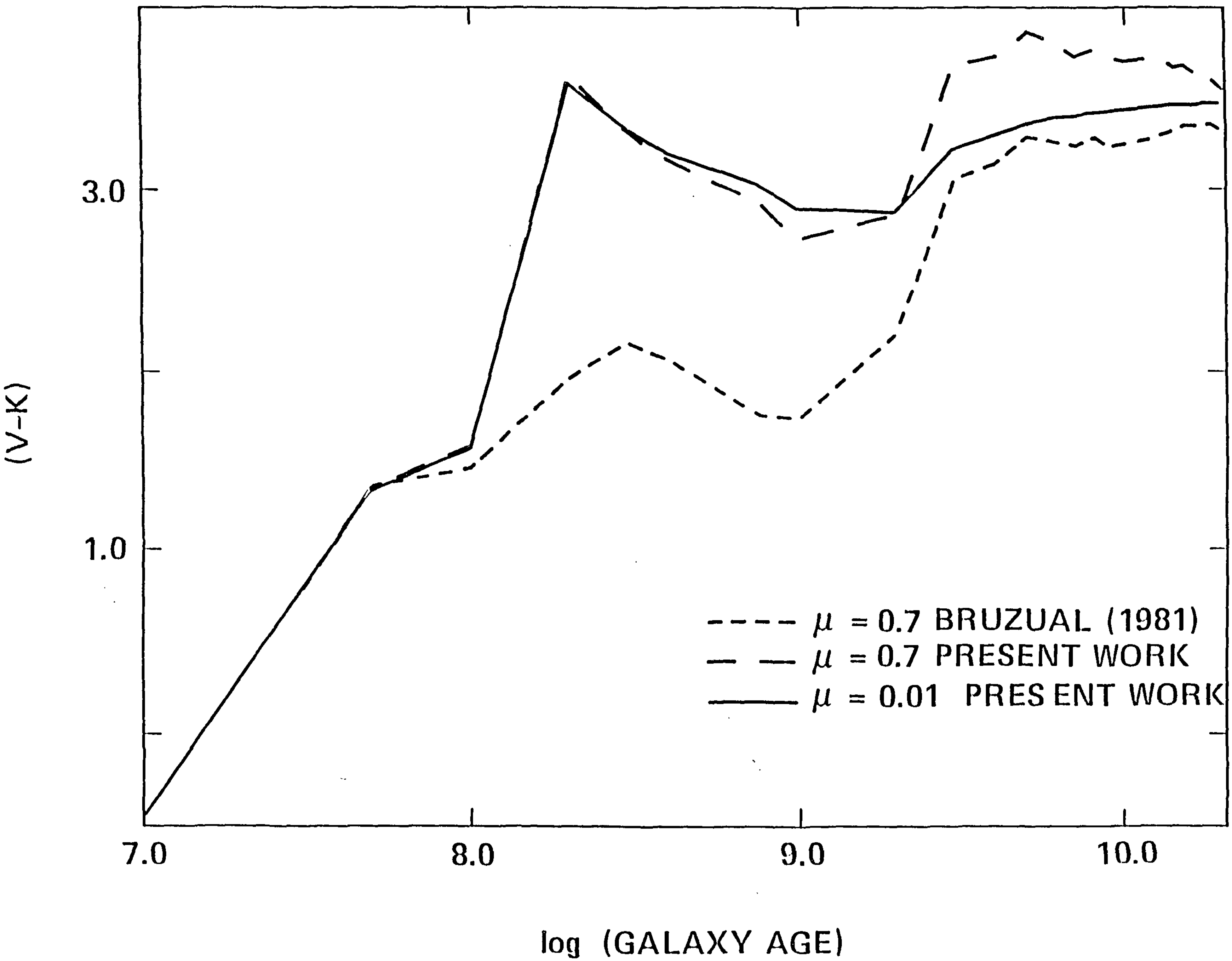

3.0
1.0
(V-K)
7.0
8.0
9.0
10.0
log (GALAXY AGE)
μ = 0.7 BRUZUAL (1981)
μ = 0.7 PRESENT WORK
μ = 0.01 PRESENT WORK

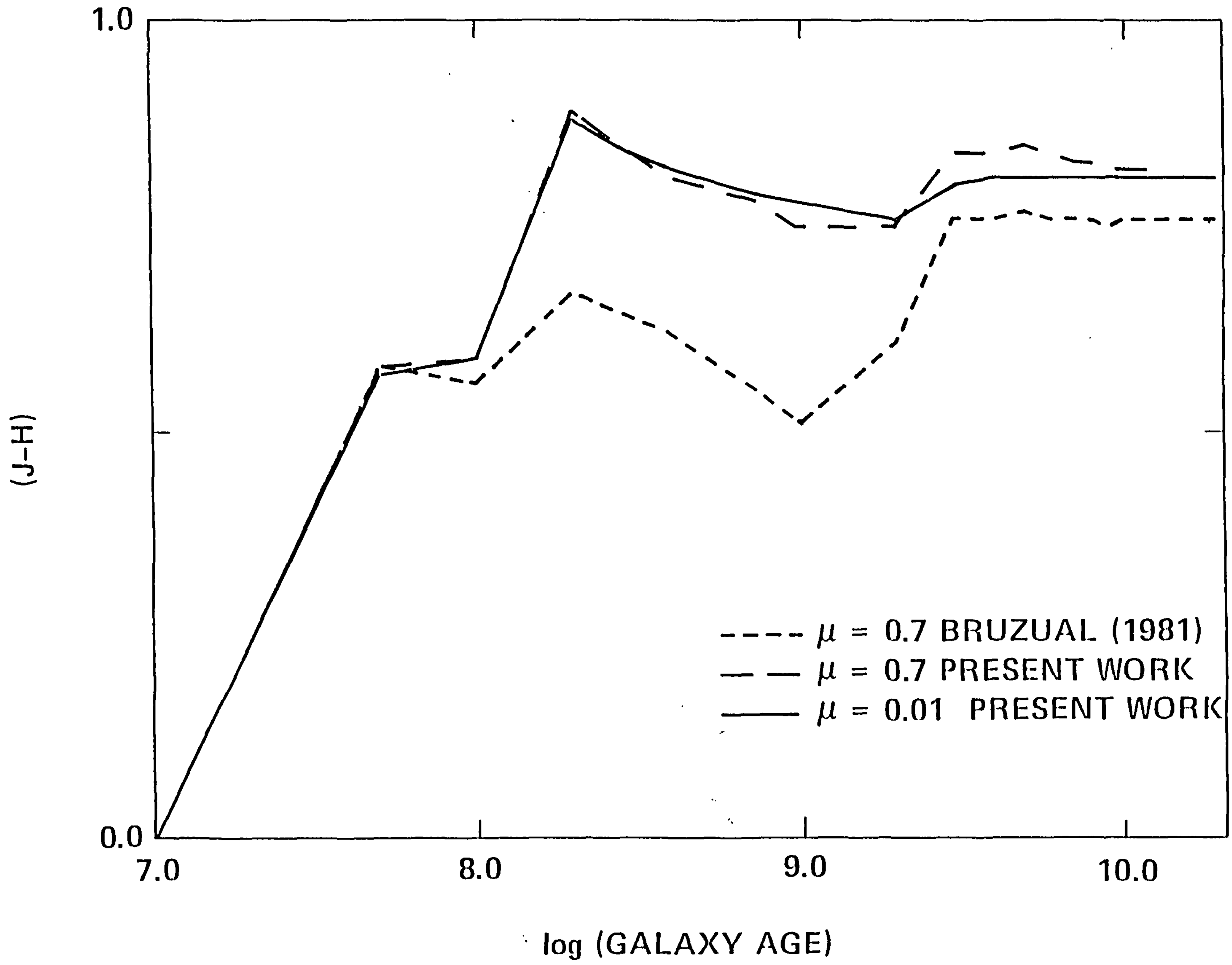
1.0
0.0
(J–H)
7.0
8.0
9.0
10.0
log (GALAXY AGE)
μ = 0.7 BRUZUAL (1981)
μ = 0.7 PRESENT WORK
μ = 0.01 PRESENT WORK

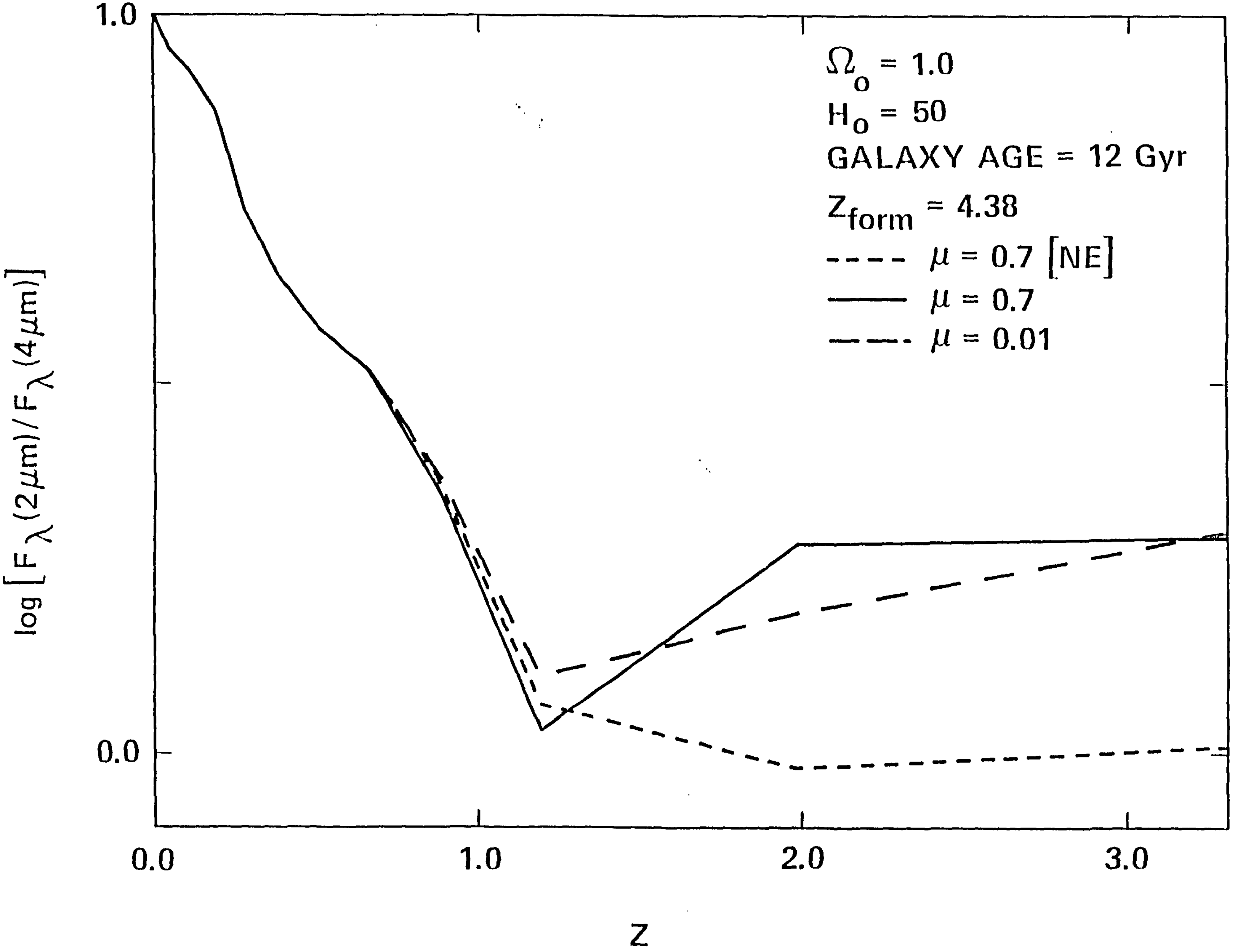

1.0
0.0
0.0
1.0
2.0
3.0
Z
log [F_λ(2μm)/F_λ(4μm)]
Ω_o = 1.0
H_o = 50
GALAXY AGE = 12 Gyr
Z_form = 4.38
μ = 0.7 [NE]
μ = 0.7
μ = 0.01

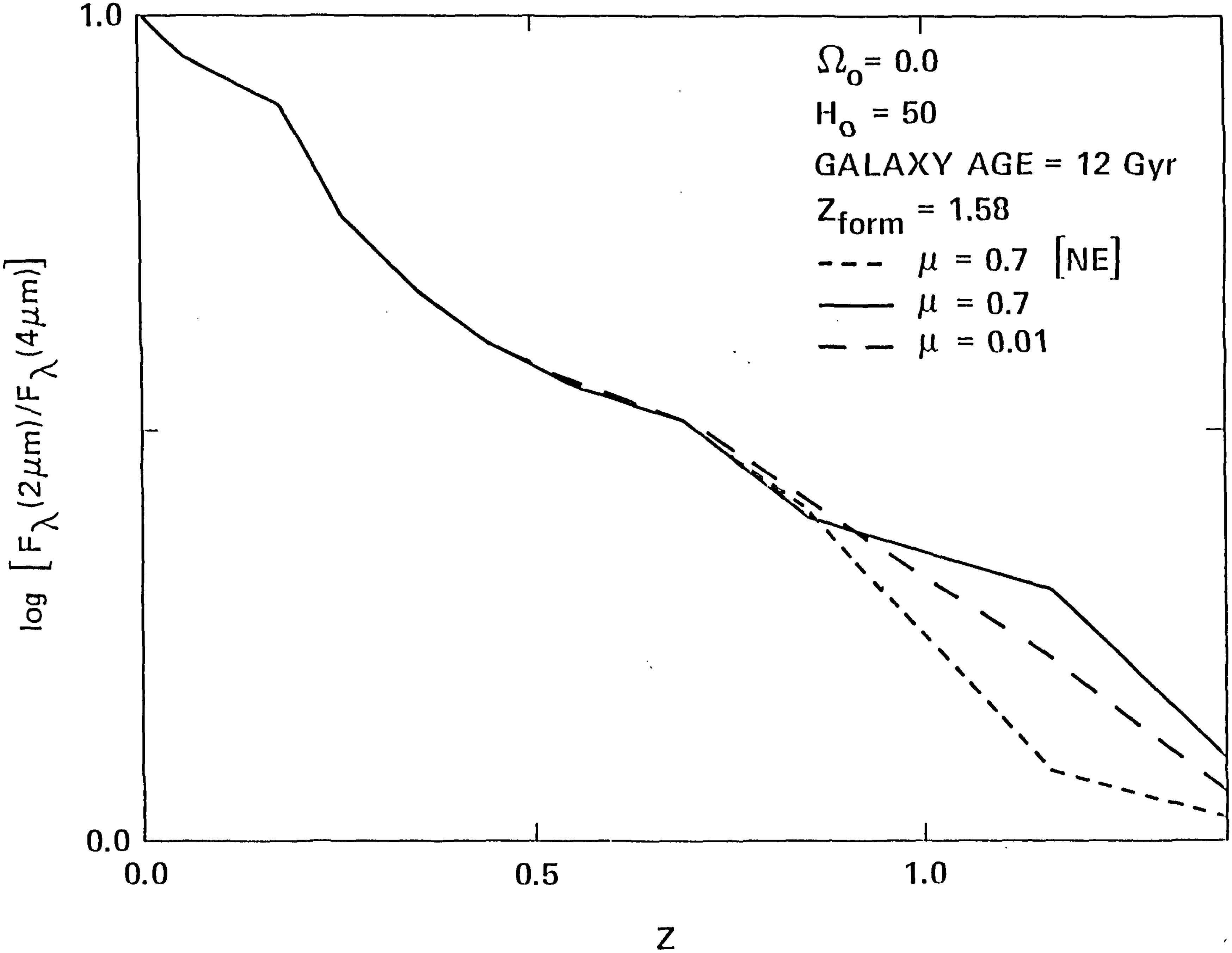

1.0
0.0
0.0
0.5
1.0
Z
log [F_λ(2μm)/F_λ(4μm)]
Ω_o = 0.0
H_o = 50
GALAXY AGE = 12 Gyr
Z_form = 1.58
μ = 0.7 [NE]
μ = 0.7
μ = 0.01

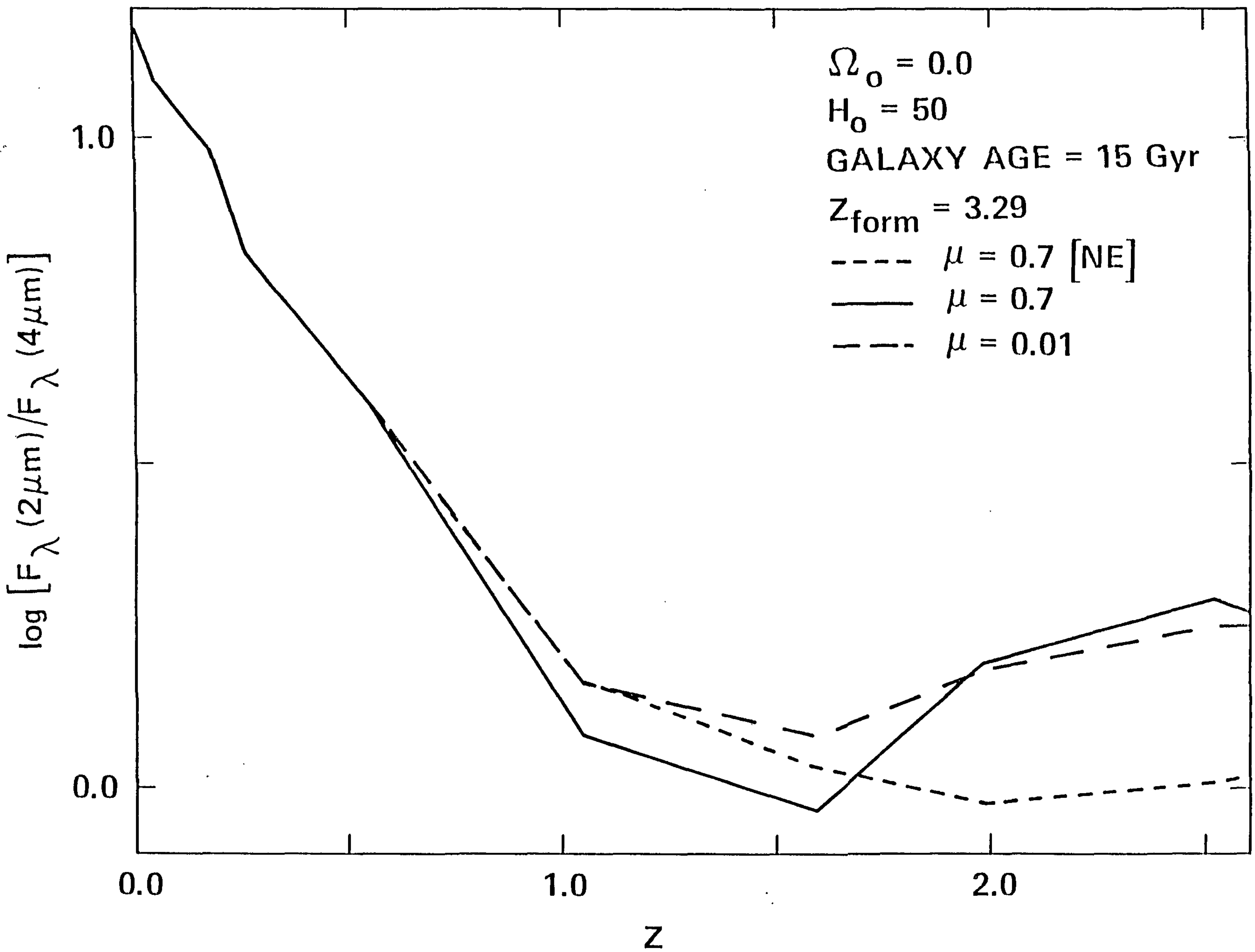

$\Omega_o = 0.0$
$H_o = 50$
GALAXY AGE = 15 Gyr
$Z_{form} = 3.29$
$\mu = 0.7$ [NE]
$\mu = 0.7$
$\mu = 0.01$
1.0
0.0
0.0
1.0
2.0
Z
$\log [F_\lambda(2\mu m)/F_\lambda(4\mu m)]$

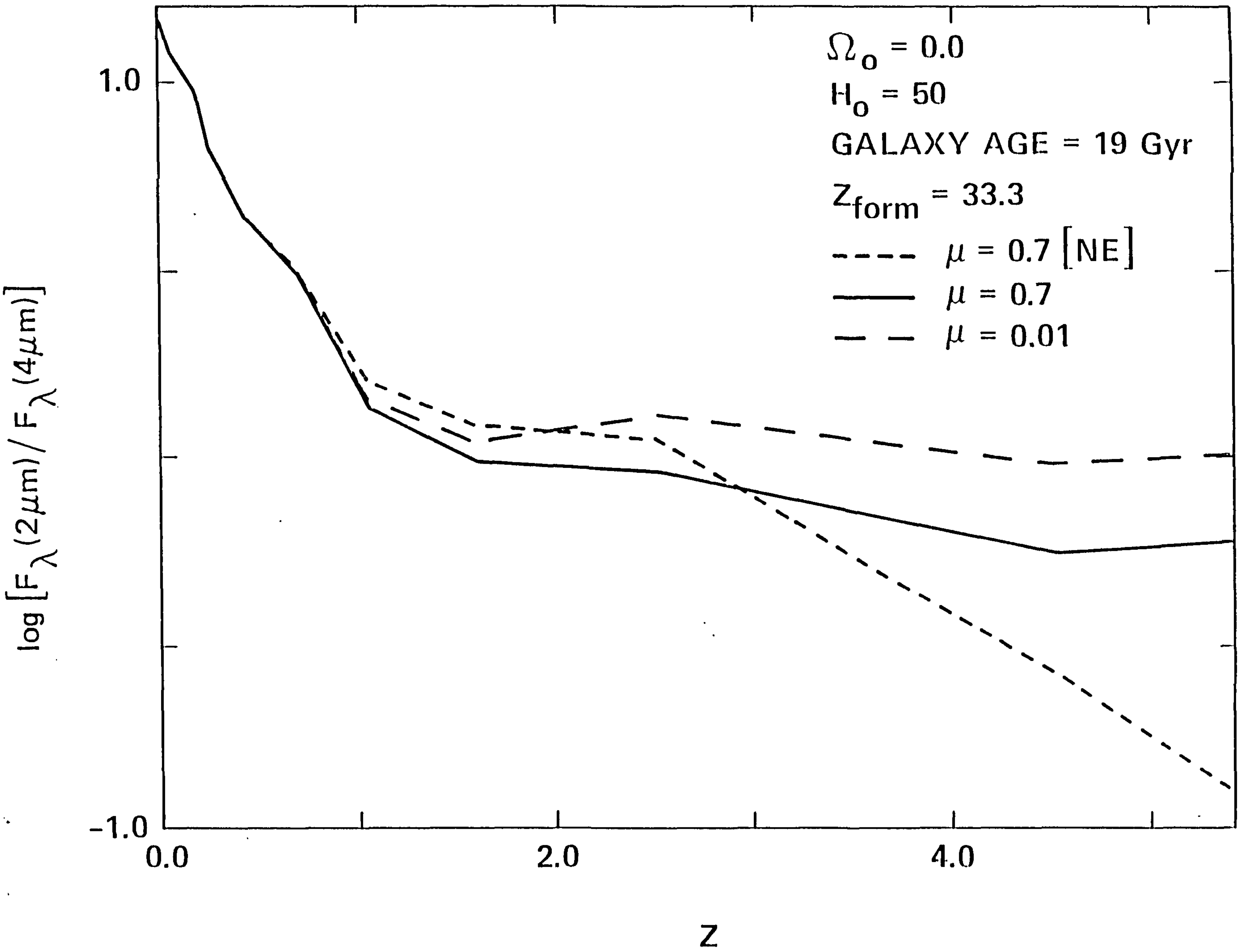

$\Omega_o = 0.0$
$H_o = 50$
GALAXY AGE = 19 Gyr
$Z_{form} = 33.3$
$\mu = 0.7$ [NE]
$\mu = 0.7$
$\mu = 0.01$
1.0
-1.0
0.0
2.0
4.0
Z
$\log [F_\lambda(2\mu m) / F_\lambda(4\mu m)]$

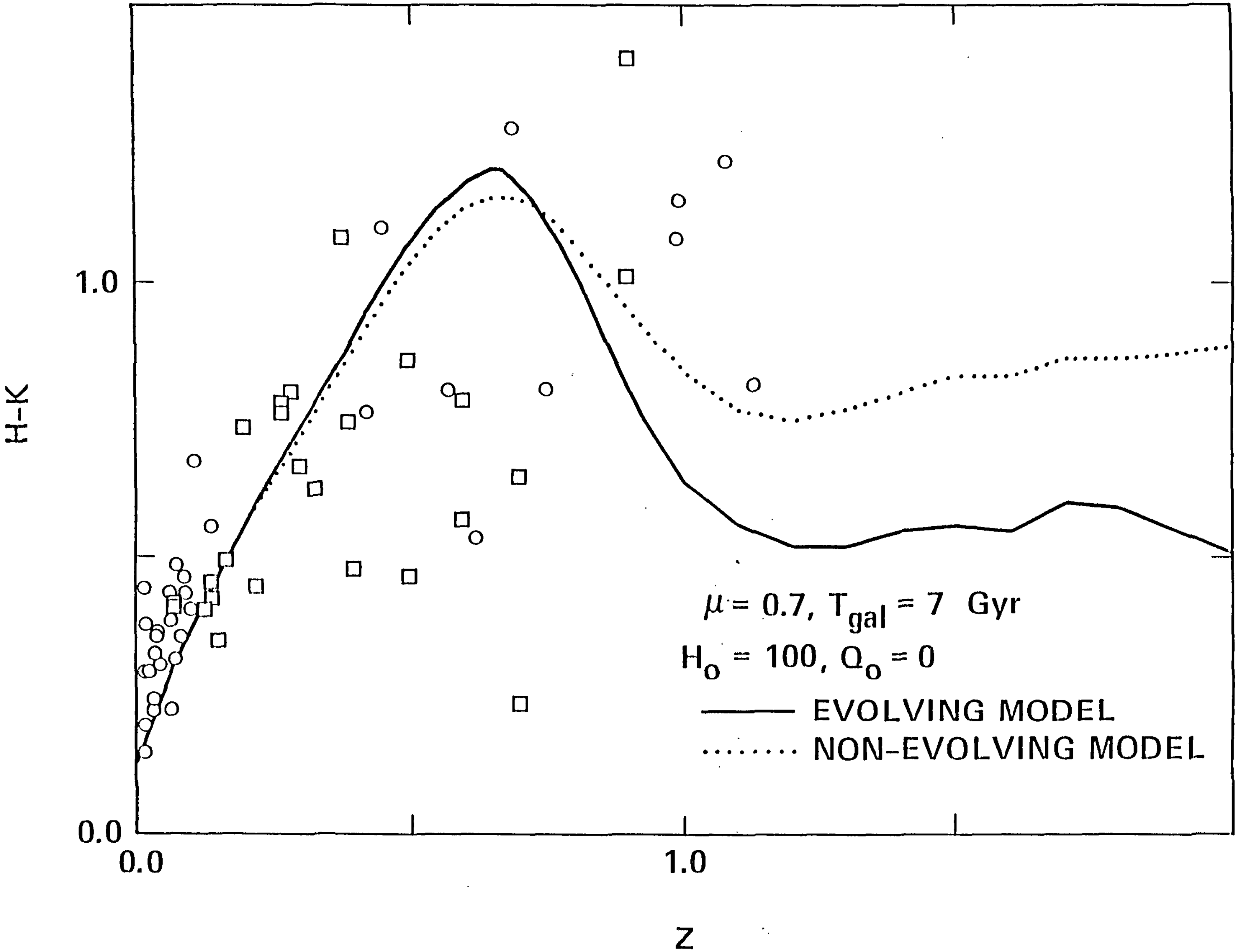

H-K
1.0
0.0
0.0
1.0
Z
μ = 0.7, T_gal = 7 Gyr
H_o = 100, Q_o = 0
EVOLVING MODEL
NON-EVOLVING MODEL

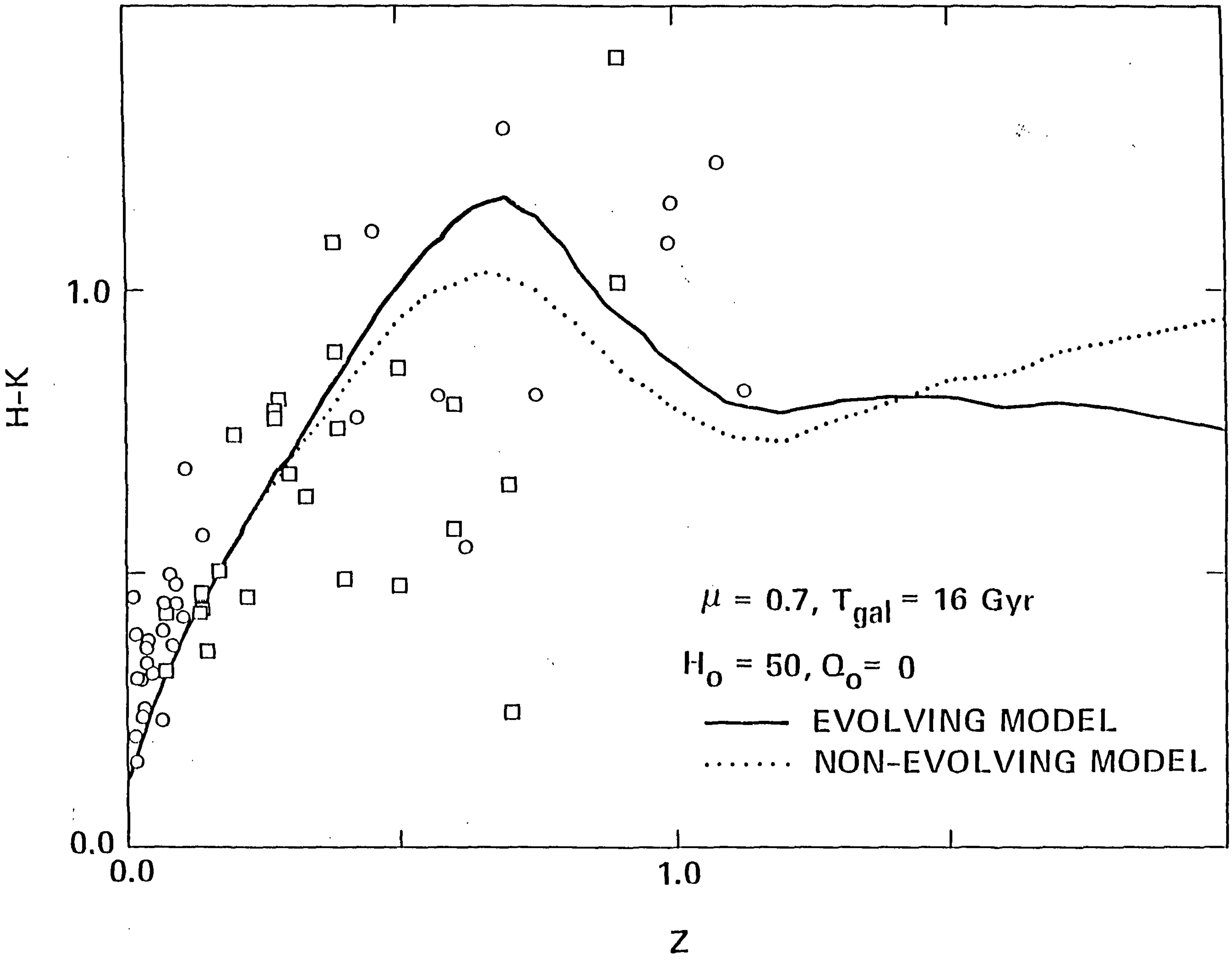

H-K
1.0
0.0
0.0
1.0
Z
μ = 0.7, T_{gal} = 16 Gyr
H_o = 50, Ω_o = 0
EVOLVING MODEL
NON-EVOLVING MODEL